# PHOTOCATALYTIC DEGRADATION OF TEXTILE DYE EFFLUENT USING CATALYST $TiO_2$/DOPED $TiO_2$

Thesis submitted in partial fulfillment of the requirement for the award of

degree of

**Master of Technology**

**in**

**Chemical Engineering**

**by**

**Alok Garg**
(Roll No. 650911001)
**UNDER THE GUIDANCE OF**

**Dr. P.K Bajpai**
**Distinguished Professor**

**Mr. V. K. Sangal**
**Assistant Professor**

**Department of Chemical Engineering**
**Thapar University, Patiala**

**Department of Chemical Engineering**
**Thapar University**
**Patiala-147004, Punjab, India**

**July 2012**

DEPARTMENT OF CHEMICAL ENGINEERING
THAPAR UNIVERSITY
PATIALA-147004 [PUNJAB]

Date: 13-07-2012

# DECLARATION

I hereby declare that the work embodied in dissertation entitled "***Photocatalytic Degradation of Textile Dye Effluent using Catalyst $TiO_2$/Doped $TiO_2$***" is original piece of work and was conducted in the Department of Chemical Engineering, Thapar University, Patiala. The matter presented in this thesis has not been submitted in part or full, to this or any other University/Institute for any degree or diploma.

Date:- 13-07-2012

Alok Garg
(Roll no.650911001)

**DEPARTMENT OF CHEMICAL ENGINEERING**
**THAPAR UNIVERSITY**
**PATIALA-147004 [PUNJAB]**

Date: 13-07-2012

# CERTIFICATE

This is to certify that the dissertation entitled, ***"Photocatalytic Degradation of Textile Dye Effluent using Catalyst $TiO_2$/Doped $TiO_2$"***, is an authentic work carried out by Mr. Alok Garg student of M.Tech. (Chemical Engineering) Thapar University, Patiala, during the year 2009 - 2012, in partial fulfillments for the award of the Degree of Master of Technology and that the dissertation has not formed the basis for the award previously of any degree, associate ship, fellowship or any other similar title to any other university or institute.

It is certified that the above statement made by the student is correct to the best of our knowledge and belief.

13-07-2012

Dr. P.K.Bajpai
Distinguished Professor
Department of Chemical Engineering
Thapar University, Patiala.

Mr. V. K. Sangal
Assistant Professor
Department of Chemical Engineering
Thapar University, Patiala

Counter signed by:

16.07.2012

Head
Department of Chemical Engineering
Thapar University, Patiala

Dean of Academic, Affairs
Thapar University, Patiala

## ACKNOWLEDGEMENTS

It is matter of immense pleasure to acknowledge my indebtedness to my Supervisor **Dr. P. K. Bajpai**, Distinguished Professor, Department of Chemical Engineering, Thapar University, Patiala and **Mr. V. K. Sangal**, Assistant Professor, Department of Chemical Engineering, Thapar University, Patiala. It is because of his priceless intellectual guidance, innovative and constructive ideas for having given me complete independence, affectionate encouragement to put my desire and thought, which paved the way for the successful completion of this work. It is indeed my privilege to work under him.

I express my special regards to **Dr. Rajeev Mehta**, Associate Professor and Head, Department of Chemical Engineering, Thapar University, Patiala for his ever helping attitude during the course of this project work.

I cannot forget to express my warmest thanks to **Dr. D. Gangacharyulu**, Professor Department of Chemical Engineering, Thapar University, Patiala for this support to start my degree.

I take this opportunity to thank Mr. Devendra Kumar, Dr. R. K. Gupta, Dr. H. Bhunia, Dr. S. Barman, Mr. Parminder Singh, Dr. J. P. Kushwaha and Dr. Avinash Chandra for their help and moral support.

I am also thankful to all faculty members and lab staff of Department of Chemical Engineering, Thapar University, Patiala for giving me support to carry put this work.

Deep heartedly, I thank my parents and my family members for their encouragement, blessings and motivation at each and every step.
Last, but not least, I thank **God** for giving me strength to overcome difficulty, which crossed my way to be a pole star.

***Thank you for making this a reality.***

**Alok Garg**

# ABSTRACT

Textile dye (reactive black 5) is example of water contaminants that are difficult to degrade by physicochemical and/or biological methods in water. Photocatalytic oxidation process has been examined to degrade reactive black 5 dye in this work. Undoped and $Fe^{3+}$ doped $TiO_2$ have been examined for such purposes. UV light with undoped TiO2 and visible light with doped $TiO_2$ can be used for degradation of reactive black 5 dye, giving $CO_2$ and $H_2O$ as final products. Visible light was successfully used to degrade reactive black 5 using Fe-$TiO_2$. It was noticed that the degradation was also depended on catalyst dose, initial concentration of contaminants and pH of dye solution. Recovered and reused $TiO_2$ catalyst showed lower activity than fresh ones. The activity loss is due to adsorption of dye on catalyst surface.

$TiO_2$ doped with $Fe^{3+}$, designated as Fe-$TiO_2$ was prepared via wetness impregnation method. The resulting products were characterized by X-ray diffraction, scanning electron microscopy, and UV-vis absorption. Experimental results revealed that for dye degradation under UV light using undoped $TiO_2$, the optimum parameters were pH = 6, $TiO_2$ = 1 $gl^{-1}$ and initial dye concentration = 100 ppm. Reaction rate constant was found to be 0.0127 $min^{-1}$ for the first order reaction kinetics. Results showed that the used catalyst was active giving 95% degradation of the dye after the first cycle and it reduced to 63 % after sixth cycle.

The results from this work showed that doping with metal ions could turn the inert amorphous $TiO_2$ to become photocatalytically active under visible light. The doping was done for three concentrations of $Fe^{3+}$ (2 %, 4% and 6% by weight). Results showed that the degradation increases as the amount of $Fe^{3+}$ increases in dopant. This indicates the importance of doped and undoped $TiO_2$ catalyst in dye degradation processes.

# *Table of Contents*

# *List of Figures*

# *List of Tables*

# Chapter-1

# INTRODUCTION

Environmental pollution and destruction on a global scale are issues of increasing concern in today's society. The presence of several organic pollutants results in a serious environmental problem. Dye pollutants from the textile industry are an important source of environmental contamination. Large quantities of dyes are extensively used in the fundamental processing steps of textile industries. It is estimated that 1-15 % of the dye concentration is lost during the dyeing processes and is released as wastewater (Zainal *et al*., 2005). The colour is usually the first contaminant to be recognized in wastewater, which is generated by using synthetic dyes in the industries. Considering both volumes discharged and effluent compositions, the wastewater generated by the textile industry is rated as one of the most polluting among all industry sectors. Given the great variety of fibers, dyes, process aids and finishing products in use, the textile industry generated wastewater of great chemical complexity, diversity and volume (Bizani *et al*., 2006).

Synthetic dyes are extensively used in the textile industries because of their simple dyeing procedure and good stability during washing process. Synthetic dyes, classified by their chromospheres, have different and stable chemical structures to meet various colouring requirements (Toor *et al*., 2006). The release of the wastewater into the ecosystem, for instance, as much as many million gallons discharged per year to waste water treatment systems, is a dramatic source of aesthetic pollution, eutrophication, and perturbation in aquatic life. Therefore, the removal of coloured wastewater is necessary before being released to the environmental (Sauer *et al*., 2002).

The traditional techniques used for colour removal are filtration, adsorption on activated carbon (charcoal), and coagulation. Each method has its advantages and disadvantages. For example, the use of charcoal is technically easy but has high waste disposal cost. Coagulation using alums, ferric salts or lime is a low cost process, but all these methods have a major disadvantage of simply transferring the pollutants form one phase to another phase rather than destroying them and sometime the byproducts may be more toxic than the dye itself. Biological treatment is a proven method and cost effective. However, it has been reported that majority of dyes are adsorbed on the sludge and require very long

degradation times, due to the biorecalcitrant nature of these dye molecules. This leads to search for highly effective method to degrade the dye into environmentally compatible products (Toor *et al*., 2006).

## 1.1 Physicochemical Methods for Waste Water Treatment

Typically, textile wastewaters have high biological oxygen demand/chemical oxygen demand (BOD/COD), a substantial proportion of which is represented by substances present in a highly emulsified and/or soluble form. The organic polluting load can be many times greater than that in ordinary domestic sewage and can also be highly coloured. A number of pretreatment processes such as equaling/ balancing, gravity adsorption or neutralization are available, and actual treatment can be achieved by chemical oxidation, ultra filtration, adsorption, and biological or physicochemical techniques.

Selection of the appropriate method of treatment is influenced by a large number of factors related to each effluent characteristic, such as relative costs, levels of treatment required or site restrictions, etc. For example biological and physicochemical treatments are often used in cycle to obtain maximum removal of organics in textile wastewater. The dual use of methods for certain organics that are not biodegradable, as well as other organic constituents that may not be variable to chemical precipitation.

### 1.1.1 Physical methods

#### *1.1.1.1 Adsorption*

Adsorption techniques have gained favour recently due to their efficiency in the removal of pollutants too stable for conventional feasible. Decolourisation is a result of two mechanisms; adsorption and ion exchange, and is influenced by many physiochemical factors, such as dye absorbent, interaction, sorbent surface area, area size, temperature, pH and contact time.

#### *1.1.1.2 Membrane filtration*

This method has the ability to clarify, concentrate and most importantly, separate dye continuously from effluent. It has some special features unrivalled by other methods; resistance to temperature, an adverse chemical environment and microbial attack. The concentrated residue left after separation, poses disposal problems and high capital cost,

and possibility of clogging and membrane replacement are its disadvantages. This method of filtration is suitable for water recycling within a textile dye plant, if the effluent contains low concentrations of dyes, but it is unable to reduce the dissolved solid content, which makes water re-use a difficult task.

### 1.1.2 Chemical methods

#### *1.1.2.1 Oxidative process*

This is the most commonly used method for decolourisation by chemical means. This is adopted mainly due to its simplicity of application. The main oxidizing agent is usually hydrogen peroxide. This agent needs to be activated by some means, for example ultra violet light. Chemical oxidation removes the dye containing effluent by oxidation in aromatic ring cleavage of the dye molecules.

#### *1.1.2.2 Photo chemical process*

This method degrades dye molecules into carbon dioxide and water by UV treatment. Degradation is caused by the production of high concentrations of hydroxyl radicals. UV light may be used to activate chemicals, such as hydrogen peroxide and the rate of removal is influenced by the intensity of the UV radiation, pH, dye structure and the dye bath composition. This may be set-up in a batch or continuous column unit. The advantage of this process is elimination of sludge and significant reduction in foul odours.

#### *1.1.2.3 Ion exchange process*

Ion exchange has not been widely used for the treatment of dye-containing effluents, mainly due to the opinion that ion exchangers cannot accommodate a wide range of dyes. Wastewater is passed over the ion exchange resin until the available exchange sites are saturated. Both cationic and anionic dyes can be removed from dye-containing effluent in this way. Advantages of this method are no loss of absorbent on regeneration, reclamation of solvent after use and the removal of soluble dyes and the major disadvantage is its high cost. This method is not effective for disperse dyes.

### 1.1.2 Physicochemical treatment

Another problem for the textile industry is the disposal of spent dye bath liquors or the combined effluent containing them. Associated with the spent dyes may be residues from

other processing aids employed in the textile finishing process. These effluents show a high degree of polluting strength as evidenced by their intense colour and high BOD/COD. Physicochemical treatment is applied either to the crude effluent or following initial biological treatment, e.g. activated sludge. Essentially, the process involves the use of a coagulating agent followed by the addition of a bridging flocculant, and finally dissolved air flotation. Almost complete colour removal can be achieved with greater than 50% reduction in COD.

#### *1.1.3.1 Precipitation/coagulation*

Effluent will contain impurities in dissolved, colloidal and suspended forms. The first stage of treatment involves the precipitation and coagulation of these impurities to produce microflocs, either by pH adjustment, or by inorganic coagulants or by organic coagulants. Organic coagulants are low molecular mass, highly charged polyelectrolyte that are usually cationic, and can be used either as an alternative to or in conjunction with inorganic coagulants.

#### *1.1.3.2 Flocculation*

When the impurities in the wastewater are in the form of microflocs and other suspended solid, the second stage of flocculation aggregates them into larger agglomerates. This is usually achieved by adding low to moderately charged polyelectrolyte with a very high molecular mass; the charge may be anionic or cationic. Flocculation involves adsorption of the polyelectrolyte onto particle surfaces. These form loops and tails which act as physical bridges across particles, thus binding them together into a polymer-particle matrix or flocs.

#### *1.1.3.3 Solid liquid separation*

This is achieved by various means, including gravity sedimentation, filtration and centrifugation. Another method gaining in popularity is dissolved air flotation, where solids are induced to float by introduction of microscopic air bubbles, which attach to the flocs and accelerate their rise to the surface. The flocks form a float, which is skimmed by mechanical scrapers in the form of sludge.

### 1.1.4 Biological Methods

#### *1.1.4.1 Anaerobic treatment*

The treatment of waste water in an anaerobic reactor converts organic materia to methane and $CO_2$. Anaerobic treatment has some advantage but it also has few disadvantages also. They are listed below:

**Advantage**

1. High loading of reactor volume
2. Reduced structural and area requirement
3. Less energy consumption
4. Process produces biogas
5. Smaller sludge generation
6. Reduced disposal cost
7. Limited nutrient addition
8. Less biological $CO_2$ generation

**Disadvantage**

1. Sensitive process of temperature, pH and loading
2. Effluent will normally require further treatment before discharge to recipient
3. Longer start-up period
4. Potential for odour problems
5. Requires higher influent concentration

Anaerobic treatment is feasible if the influent concentration is approximately 1,000 g BOD/$m^3$**.**

#### *1.1.4.2 Aerobic treatment*

Organic material is converted into $CO_2$ and sludge (biomass) throught aerobic treatment. The conversion is done with $O_2$ supplied to the reactor tank either mechanically or by diffusion from the atmosphere.

A frequent problem with activated sludge plants is the build-up of filamentous biomass, which can result in excess suspended solids in the effluents and, in the worst case, a sludge wash out.

## 1.2 Advanced Oxidation Processes for Waste Water Treatment

Advanced oxidation processes (AOPs) is the common name of several chemical oxidation methods used to remediate substances that are highly resistant the biological degradation. Although oxidation can be total, frequently a partial oxidation is sufficient to decrease the toxicity of the biorecalcitrant compound enabling their final treatment by conventional biological treatment.

The complete oxidation leads to mineralization and yields $CO_2$, and inorganic ions. The partial oxidation can be enough to decrease toxicity enabling biological degradation, but is

essential to verify if the intermediary products formed are not more toxic than the parent compound under treatment. AOPs can remediate all different types of organic pollutants in liquid, gaseous or solid media, reason why they are used on the remediation of contaminated waters, liquid or gaseous effluents and also on the treatment of different hazardous wastes namely on contaminated soils. Some of the above mentioned reviews present comprehensive compilations of the substances and residues already mineralized using different advanced oxidation processes (Blake, 2001, Legrini, et al., 1993).

### 1.2.1 Theory of advanced oxidation processes

Although different advanced oxidation processes use several different reaction systems, all of them have the same chemical characteristic: i.e., the production and use of hydroxyl radicals (OH•) (Eckenfelder, 2000; Metcalf and Eddy, 2003). Hydroxyl radicals are highly reactive species that are able to attack and destroy even the most persistent organic molecules that are not oxidized by the oxidants as oxygen, ozone or chlorine (Eckenfelder, 2000). Table 1.1 shows oxidation potential of the hydroxyl radical and compares it with others commons oxidants used in chemical oxidation (Fox and Dulay, 1993).

**Table 1.1:** Oxidation potential of most common oxidizing agents

| Oxidizing agent | Oxidation potential (Volt) |
|---|---|
| Fluorine | 3.06 |
| Hydroxyl radical | 2.80 |
| Atomic oxygen | 2.42 |
| Ozone | 2.08 |
| Hydrogen peroxide | 1.78 |
| Hypochlorite | 1.49 |
| Chlorine | 1.36 |
| Chlorine dioxide | 1.27 |
| Molecular oxygen | 1.23 |

Hydroxyl radical is the most powerful oxidant after fluorine; it is able to initiate several oxidation reactions leading to complete mineralization of the original organic substances and their subsequent degradation products. Hydroxyl radical reacts will all classes of organics mainly by hydrogen abstraction:

$$OH\bullet + RH \rightarrow R\bullet + H_2O \qquad (1.1)$$

Hydrogen abstraction produces organic radicals able to react with molecular oxygen and originating peroxyl radicals.

$$R\bullet + RH \rightarrow R\bullet + H_2O \qquad (1.2)$$

Electrophilic additions may also occur (Legrini et al., 1993).

$$OH\bullet + PhX \rightarrow HOPhX\bullet \quad (1.3)$$

Electron transfer reactions,

$$OH\bullet + RX \rightarrow RX\bullet + + OH- \quad (1.5)$$

and reactions between hydroxyl radicals,

$$2OH\bullet \rightarrow H_2O_2 \quad (1.6)$$

Hydroxyl radical is characterized by a non-selective attack; this is an extremely useful characteristic for an oxidant to be used on environmental remediation. Other relevant and important characteristics are the existence of several possible pathways for hydroxyl radical production and the fact that all reactions occur at normal temperature and pressure. AOPs advantageously promote complete degradation of pollutants being remediated while classical treatments usually only transfer target pollutants to another phase, leading to the production of secondary residues (slugs) that require further treatment or deposition. Therefore, the advanced oxidation process is a good method for environmental decontamination (Linsebigler et al., 1995).

AOPs versatility is favoured also by the existence of various pathways to produce hydroxyl radicals, which enables a high adaptability to any specific environmental remediation problem. The advanced oxidation process can degrade all types of organic compounds in water therefore they are widely used in industrial wastewater remediation.

### 1.2.2 Processes used in the production of hydroxyl radicals

Advanced oxidation processes enclose several different treatments options: as ozone, hydrogen peroxide, ultraviolet radiation, ultrasound, homogeneous and heterogeneous photocatalysis, photocatalytic disinfection and also their combination (Hoffmann et al., 1995). The use of hydroxyl radicals to promote chemical oxidation it is the common feature of all AOPs. Table 1.2 shows several of the chemical oxidation technologies available. The AOPs classification is frequently based on the use or not of ozone on the production of hydroxyl radicals. The classification can also be based on the use or not of irradiation and on the number of phases (homogeneous or heterogeneous).

**Table 1.2:** Processes used in the production of hydroxyl radicals (Metcalf and Edyy, 2003)

| Processes with ozone | Processes without ozone |
|---|---|
| Ozone at high pH (8-10) | $H_2O_2$ + UV |
| Ozone + UV | Photocatalysis (UV+ photocatalyst) |
| Ozone + $H_2O_2$ | Ultrasound |
| Ozone + $H_2O_2$ + UV | Oxidation supercritical |
| Ozone + $TiO_2$ | $H_2O_2$ + UV + iron salts (Foto-Fenton) |
| Ozone + $TiO_2$ + $H_2O_2$ | $H_2O_2$ + iron salts (Fenton reagent) |
| Ozone + ultrasound | |

Ozone + UV, ozone + hydrogen peroxide, ozone + UV + hydrogen peroxide and hydrogen peroxide + UV are the most used commercial processes and its use will be analyzed below (Metcalf and Edyy, 2003). Brief description, advantages and disadvantages of few AOPs discussed in Table 1.3.

Advanced oxidation processes (AOPs) hold several advantages in the field of waste water treatment:

- It could effectively eliminate organic compounds in aqueous phase, rather than collecting or transferring pollutants into another phase.
- Due to the remarkable reactivity of $OH\cdot$, it virtually reacts with almost every aqueous pollutants without much discrimination. AOPs could therefore be applicable in many, if not all, scenarios where many organic contaminants are expected to be removed at the same time.
- Some heavy metals could also be removed in forms of precipitated $M(OH)_x$.
- In some AOPs designs, disinfection could also be achieved, leading AOPs to an integrated solution to some of the water quality problems.
- The complete reduction product of $OH\cdot$ is $H_2O$, AOPs theoretically do not introduce any new hazardous substances into the water.

**Table 1.3** Brief description, advantages and disadvantages of AOPs

| AOP technology | Brief description | Advantages | Disadvantages |
|---|---|---|---|
| **General AOPs** | Oxidation of organic contaminants occurs primarily through reactions with highly reactive radical such as OH•. The formation of these radicals can occur through several different processes that are discussed below. | • AOPs are destructive processes.<br>• Several AOPs have disinfectant capabilities.<br>• Many AOP components have been utilized in the water community and industry. | • Potential for accumulation of oxidation by-products.<br>• Potential for bromated formation.<br>• Radical scavenging by interfering compounds can reduce effectiveness of AOPs. |
| **$H_2O_2/O_3$** | When $O_3$ and $H_2O_2$ are simultaneously applied to water, they react to form hydroxyl radicals. These OH• can oxidize most dissolved organic matter to form by-products. | • Efficient treating waters with high organic matter concentrations.<br>• Supplemental disinfectant.<br>• More effective than $O_3$ or $H_2O_2$ alone.<br>• Established technology for remediation applications. | • Potential for bromated formation (controllable through adjustment of $O_3/H_2O_2$ ratio and pH).<br>• Many require to treatment of excess $H_2O_2$ due to potential for microbial growth.<br>• Many require ozone off-gas treatment and/or permitting. |
| **$O_3$/UV** | Hydroxyl radicals are generated when low-pressure UV light is applied to ozonated water. Destruction of organic compounds occurs by hydroxyl radicals reactions, coupled with direct photolysis and oxidation by molecular ozone. | • Supplemental disinfectant.<br>• More effective than $O_3$ or UV alone.<br>• More efficient at generating OH• than $H_2O_2$/UV process for equal oxidant concentrations. | • Energy and cost intensive process.<br>• Potential for bromated formation (controllable through adjustment of $O_3/H_2O_2$ ratio and pH).<br>• Turbidity can interface with UV light penetration.<br>• Ozone diffusion can result in mass transfer limitations.<br>• May require ozone off-gas treatment and/or permitting.<br>• Interfering compounds (e.g., nitrate) can absorb UV light.<br>• UV lamp and sleeve failure can potentially |

| | | | |
|---|---|---|---|
| | | | contaminate water with mercury. |
| **$H_2O_2$/UV** | As in the $O_3$/UV process, several synergistic oxidation mechanisms result in the destruction of organics. The OH• radical route is the predominant removal mechanism. For $H_2O_2$ a greater number of radicals are produced when MP-UV lamps are used compared to the LP- UV lamps. | • No potential for bromate formation.<br>• Can oxidize >95% organic matter compared to <10% for UV or $H_2O_2$ alone.<br>• MP-UV and pulsed-UV irradiation can serve as disinfectant.<br>• No off-gas treatment required.<br>• Not limited by mass transfer relative to $O_3$ processes. | • Turbidity can interfere with UV light penetration.<br>• Less stoichiometrically efficient at generating OH• than $O_3$/UV process<br>• Interfering compounds (e.g., nitrate) can absorb UV light.<br>. |
| **Sonication / Hydrodynamic Cavitation** | Sonication or hydrodynamic processes induce the formation of cavitation micro bubbles. These bubbles implode violently after reaching a critical resonance size and generate high temperatures and highly reactive radicals. Removal of organics occurs by thermal decomposition at the bubble- water interface and by reaction with the radicals. Oxidation by cavitation is enhanced by the addition of $O_3$ or $H_2O_2$ . | • Simple design resulting in minimal maintenance costs.<br>• Energy usage comparable to AOPs using UV.<br>• No bromate formation potential if $O_3$ is not added.<br>• Less heat transfer relative to UV system.<br>• No off-gas treatment required if $O_3$ is not used. | • No full-scale applications exist.<br>• Supplemental oxidants such as $O_3$ and $H_2O_2$ may be required to achieve target removal efficiencies, resulting in increased costs. |
| **$TiO_2$ Catalyzed UV oxidation** | When $TiO_2$ is illuminated by UV light, valence band electrons are excited to the conduction band, resulting in the formation of holes. These holes react with | • No potential for bromate formation.<br>• Can be performed at higher (300- 380 nm) wavelengths than other UV oxidation processes.<br>• No off-gas treatment | • No full-scale applications exist.<br>• Pre-treatment necessary to avoid fouling of the $TiO_2$ catalyst.<br>• If $TiO_2$ is added as slurry, then a |

| | | | |
|---|---|---|---|
| | water molecules to produce hydroxyl and other radicals that in turn oxidize organic compounds. Formation of $H_2O_2$ intermediate can also assist the overall oxidation process. | required. | separation step is required.<br>• Potential for rapid loss of $TiO_2$ activity, requiring catalyst on-site storage or regeneration method.<br>• Rigorous studies needed to determine the optimum $TiO_2$ dose.<br>• May require oxygen sparging.<br>• Reaction efficiency is highly pH- dependent, requiring close monitoring and control. |
| **Fenton's Reaction** | Radicals, including OH• are produced when Fe (II) reacts with $H_2O_2$. Destruction of organic matter occurs by reaction with these radicals. Iron acts as a catalyst for this reaction. | • No potential for bromate formation.<br>• Not an energy intensive process compared to AOPs that utilize $O_3$ or UV.<br>• No off-gas treatment required. | • No full-scale applications exist.<br>• Requires iron extraction system.<br>• Very low pH (<2.5) is required to keep the iron in solution.<br>• pH adjustment will increase operation and maintenance costs. |

In recent years, there has been an extensive interest in heterogeneous photocatalysis using semiconductors for the treatment of recalcitrant chemicals present in the wastewater. The main advantage of this method is that the pollutants are destroyed with no requirement for secondary disposal of concentrated wastes, providing a more environmentally sustainable solution. Among the semiconductors being studied are $TiO_2$, ZnO, $Fe_2O_3$, CdS, and ZnS. $TiO_2$ has been successfully used to decolourize and mineralize many organic pollutants including several dyes and their intermediates present in aqueous systems using both artificial light and under sunlight using solar technology (Muruganandham *et al*., 2005).

$TiO_2$ is the most widely used photocatalyst because of its good activity, chemical stability, commercial availability. It is generally used as a photocatalyst for environmental

applications such as air purification, water disinfection, hazardous waste remediation and water purification (Nagaveni *et al*., 2004). However, $TiO_2$ is active only under ultraviolet light (UV) because of its wide band gap, ~3.2 eV for anatase and ~3.0 eV for rutile, and high rate of recombination of photogenerated electron hole pairs resulting in low photo quantum efficiency. Several approaches have been applied to optimize the photocatalyst itself in order to improve the photocatalytic activity.

Nowadays, doping with metal ions is being attempted to improve $TiO_2$ catalyst with visible-light response because transition elements have many valences and metal ions doped in the $TiO_2$ matrix can be superficial potential trap of photogenerated electron - hole pairs, then lengthen the lifetime of electrons and holes and increase photocatalytic activity (Yang *et al*., 2004). Unfortunately, nearly all photocatalytic studies on $TiO_2$ have focused on the crystalline forms, as it is commonly accepted that amorphous $TiO_2$ contains high concentration of defects that will invariably function as rapid electron - hole pairs recombination centers to render them inactive. However, amorphous $TiO_2$ has one interesting property - the high surface area which can lead to high adsorptivity. Up to date, there have been only a few reports that studied or showed interest in amorphous $TiO_2$.

## 1.3 Objectives of the Present Study

The present work is carried out under the following objectives:

I. Study of photocatalytic degradation of reactive black 5 in presence of suspended $TiO_2$ semiconductor and UV light in slurry pond reactor.
II. Preparation & characterization of metal ion doped $TiO_2$ photocatalyst.
III. Study of photocatalytic degradation of reactive black 5 in presence of suspended metal ion doped $TiO_2$ semiconductor and visible light in slurry pond reactor.

# Chapter-2

## LITERATURE REVIEW

Textile dyes are examples of water contaminants that are difficult to degrade by physicochemical and/or biological methods in water. Photocatalytic oxidation process has been examined to degrade reactive black 5 dye.

In this chapter, the essential issues of photo-catalysis in semiconductor materials will be discussed, and will focus on the different aspects of $TiO_2$ photocatalyst. Some factors which manipulate the efficiency of the photo-catalytic process, including the different properties of the photocatalyst will be briefly discussed. The mechanistic aspects of photo-oxidation of some organic compounds in aqueous system will also be considered. There are some limitations on application of $TiO_2$ photocatalyst in large scale application. Investigations have been made modifying the photocatalyst to get good photo-activity in the visible light irradiation. These modification techniques are discussed mainly to produce $TiO_2$ photocatalyst in the form of powder or nanoparticles. The studies of other modification methods will also be discussed to give a comparative approach. Furthermore, some previous research has been reported for the use of $TiO_2$-based photocatalysts that were used in the visible light photo-degradation of organic pollutants.

Many investigations have been conducted to find out the prospective applications of photocatalyst in different areas. For example, the use of thin film $TiO_2$ for self-cleaning surfaces has been commercialized in Japan (Fujishima *et al.,* 1999). Several studies have been done on the production of hydrogen through water splitting reaction by using semiconductor photocatalysts. It shows potential as an alternative energy in the future (Anpo and Takeuchi, 2003). Other studies have been done in the areas of photocatalysis for the use photocatalysts to oxidize toxic and organic pollutants in water treatment or waste water treatment.

Due to many reasons $TiO_2$ or $TiO_2$-based photocatalysts are widely used as compared to other semiconductor photo-catalyst (ZnO, $WO_3$, CdS, ZnS, $SrTiO_3$, $SnO_2$, and $Fe_2O_3$). $TiO_2$ or $TiO_2$-based photocatalysts are non-toxic, and have highly oxidizing potential and high chemical strength. In the application of organic pollutant photo-degradation, $TiO_2$ photocatalysts have been the most active compared to other semiconductors (Cunningham

*et al.,* 1999). They may be used in the form of particle suspension or colloid, highly dispersed nanoparticles on a porous media, and also as a thin film on a supporting material.

## 2.1 Photocatalysis on $TiO_2$

In 1972, Fujishima and Honda experimented the effect of photo-degradation of the titanium dioxide ($TiO_2$) electrode on the water electrolysis into hydrogen and oxygen (Fujishima and Honda, 1972). Later on, photocatalysis by $TiO_2$ semiconductor has constantly established great awareness in order to efficiently application or convert solar light energy to perform desirable chemical reactions.

### 2.1.1 Introduction to photocatalysis

The photo-catalytic reaction is measured as a heterogeneous catalytic process. It is mostly accepted that a heterogeneous catalytic process occurs through these following seven steps:

i. mass transfer of reactants from bulk fluid to the catalyst surface (external diffusion)
ii. mass transfer of reactants from the catalyst surface into its pore structure (internal diffusion)
iii. adsorption of reactants
iv. surface reaction
v. desorption of products
vi. mass transfer of products out of the pore structure of the catalyst to the surface
vii. mass transfer of products from the catalyst surface to bulkfluid.

The IUPAC defines photo-catalysis as “the catalytic reaction involving light absorption by a catalyst or substrate” (Braslavasky and Houk, 1988). Consequently, photo-catalysis may include photoactivation of catalysts, photochemical activation of catalytic system, and catalysts of photochemical reactions (Pareek and Adesina, 2003).

Photocatalysis includes redox reactions of organic or inorganic molecules (Teichner *et al.,* 1985), induced by suitable light irradiation upon a semiconductor particle. Thus, photocatalytic reactions (equivalent to step iv surface reaction above) can be described as follows (Schiavello, 1988):

a. photogeneration of electron-hole pairs by exciting a semiconductor with radiation of suitable light energy;
b. separation of electron-hole pairs by traps which have a trapping rate higher than the electron-hole recombination rate;
c. redox reaction between the separated electrons and holes with adsorbed substrates.

In other words, some key events of kinetic processes at the surface of photoexcited semiconductor are: photoexcitation, migration and trapping of the photogenerated electrons and holes, surface charge transfer reaction between trapped electron or hole and absorbed species, and unfavorable electron-hole recombination.

### 2.1.2 Electronic excitation process in semiconductor

The semiconductor element can be motivated by absorption of photons on or near the surface of semiconductors. Semiconductors are characterized by actively non-overlapping bands (Pitchat and Fox, 1988). Thus, this photoexcitation means a band-to-band electronic transition, moving an electron from the topmost filled band (valence band) to the closest empty band (conduction band). The difference between energy level of these bands is known as band-gap energy (Figure 2.1). Irradiation by light with photon energy at or greater than the band-gap energy will lead to electron excitation, resulting in the formation of an electron/hole pair in the semiconductor particle:

$$SC + h\nu \rightarrow SC(e_{CB} + h^{+}_{VB}) \quad (2.1)$$

Where: $e_{CB}$ = a conduction band electron and $h^{+}_{VB}$ = a positive hole in valence band

The minimum wavelength of the incident radiation that is required to promote an electron excitation depends upon the band gap energy ($E_{bg}$) of the photocatalyst is given by Mills *et al.,* (1993)

$$E_{bg} = \frac{1240}{\lambda_{min}} \quad (2.2)$$

Where: $\lambda_{min}$ = the minimum wavelength (nm) of incident radiation to induce photoexcitation of a semiconductor with band gap energy $E_{bg}$ (eV).

Photogenerated electrons and holes may either recombine, dissipating energy or further move to the surface of the semiconductor to perform redox reactions with electron donor

or acceptor species adsorbed on the surface, as shown in Figure 2.2 (Mills and Hunte, 1997).

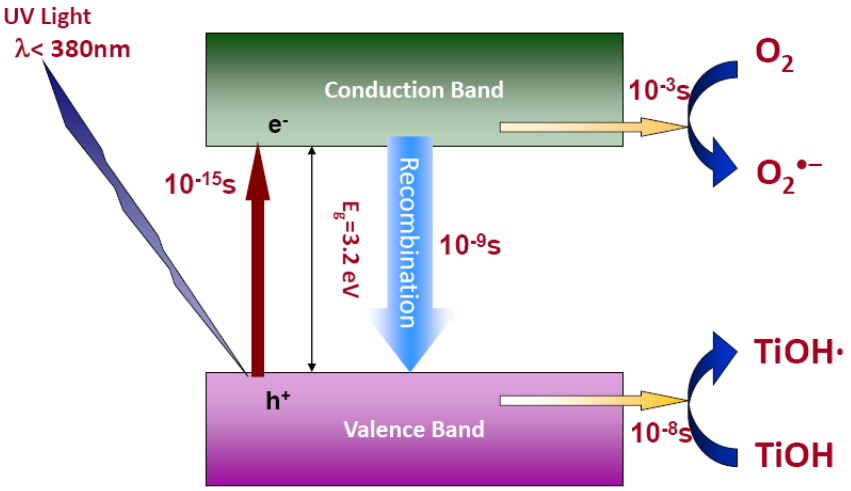


**Figure 2.1:** Energy band gap within solid semiconductor

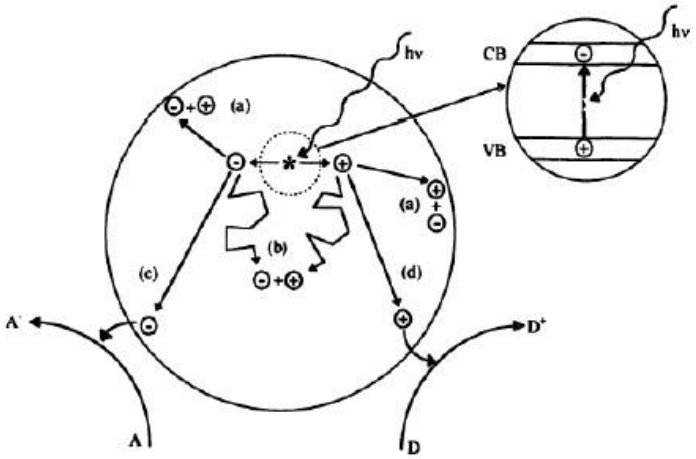


**Figure 2.2:** Major events occurring on a semiconductor particle

Electron-hole recombination may occur at the surface or in the bulk of the semiconductor. At the particle surface, photogenerated electrons can reduce an electron acceptor. Photogenerated holes can oxidize an electron donor D. Ideally, electrons and holes must be somehow separated to minimize the electron-hole recombination process. The intrinsic properties of a semiconductor determine its photocatalytic activity. These include the magnitude of the semiconductor band-gap energy, crystal configuration, surface area, porosity, and surface affinity to the hydroxyl groups (Pareek and Adesina, 2003).

### 2.1.3 Determining factors on photocatalytic process

The exterior diffusion in photocatalytic process will be affected by the fluid dynamic features of the system and interior diffusion is due to morphological and textural properties of photocatalyst particles. In general, the adsorption desorption processes and catalytic reactions will be decided by the nature of the chemical interaction between fluid and solid catalyst as well as the morphological and textural properties of the solid (Schiavello, 1988). Based on the previous explanation in section 2.1.1, the effectiveness of the photocatalytic reaction step mainly depends on:

i. successful electronic excitation;
ii. good separation of photogenerated charge carriers (electron-hole pairs);
iii. fast interfacial electron transfer, photogenerated electrons in the conduction band to be captured by adsorbed electron acceptors while photogenerated holes in the valence band to be filled by adsorbed electron donors.

The rate of photocatalytic reaction is subjected by the nature as well as concentration of contributing substrate and the extent of interaction between the 3 phases of matter (air, liquid, and solid catalyst) involved (Pareek and Adesina, 2003). The dispersed fine catalyst particles in an aqueous solution might be divided into two categories, firstly, factors that are associated with the nature of the photocatalyst and secondly, others attributed to the fluid bulk properties and these are the factors that will govern the photocatalytic process in a rector.

#### *2.1.3.1 Effect of wavelength and light intensity*

The photon energy i.e. required for electron excitation from VB to CB comes from radiation source that may be lamp or sunlight. And it is necessary that the wavelength of photon energy must have shorter than the critical wavelength, which depends on the semiconductor band-gap. In general, the total energy input to the photocatalytic process depends upon the light intensity.

Yoneyama *et al*., (1983) investigated that the rates of reaction for gases, aqueous solution, or organic liquids, are found to be directly proportional to flux of light radiation. Okamoto *et al*. (1985) and Ollis et al. (1991) reported that the photodegradation rate increased linearly at low intensities; however, at medium light intensities the rate became dependent

on the square root of light intensity and independent at high intensities. The penetration length of light in the solid-liquid medium is another important parameter, which is a function of particle size and catalyst charge or slurry concentration. In the case of artificial light, the intermediates generated are also affected by the wavelength as well as intensity of the light (Matthews and McEvoy*et al*., 1992).

### *2.1.3.2 Effect of photolysis*

In some cases, the adsorbed species may undergo a chemical transformation directly by the light irradiation. This mechanism is called as photolysis (Schiavello, 1988). The solid simply plays the role of adsorbent material. Thus, in semiconductor materials both photocatalysis and photolysis may occur at the same time.

### *2.1.3.3 Effect of catalyst loading*

Ollis *et al*., (1991) and Chen and Chou, (1993) have shown that the rate of photocatalytic degradation initially increased with catalyst loading but smoothed off at high values due to light-scattering properties. Bangun and Adesina, (1998) proposed that the photocatalytic reaction rate, $r_{rxn}$, dependency on titania catalyst concentration may be described as:

$$r_{rxn} = \frac{K_{cat}\, C_{cat}}{\left(1 + \alpha_{cat} C_{cat}\right)^2} \tag{2.3}$$

where $k_{cat}$ and $\alpha_{cat}$ are reaction parameters.

The equation above suggests that the optimum catalyst dosage is $1 / \alpha_{cat}$.

### *2.1.3.4 Effect of substrate type and concentration*

The photocatalytic degradation process is highly non-selective as over 1000 compounds have been investigated for photocatalytic destruction within the past 15 years (Blake, 1995) with $OH^-$ radical as the principal oxidizing species (Trillas *et al*., 1992 and Turchi and Ollis, 1990). However, some workers also suggested that there is a possibility for the direct oxidation by the photogenerated holes. Under constant oxygen partial pressure, Wei and Wan (1991) proposed a two site Langmuir-Hinshelwood (LH) kinetic model for phenol degradation to describe the initial rate rise followed by a plateau at high reactant concentration. However, in some cases the photocatalytic rate might decrease at high

reactant concentration due to product inhibition, as found during the photodegradation of sodium dodecyl sulfate.

Alekabi and Serpone, (1988) suggested that the photodegradation of halogenated phenol, such as 4-chlorophenol, 2, 4- dichlorophenol, and 2, 4, 5-trichlorophenol, was found to be dependent on the number of Cl atoms on the ring. The release of $Cl^-$ ions into solution was probably the cause of observed inhibition effects since Cl had strong electrophilic character and possibly competed with $O_2$ for adsorption on the photocatalyst surface. Similar observations were also suggested by other groups working with chlorinated aliphatic compounds (Hsiao et al., 1983; Pruden and Ollis1983).

In homogeneous aromatic system, the photoactivity of a compound is significantly influenced by the electronic properties of the substituents on the benzene ring (Hansch et al., 1991) and therefore, the $k_{obs}$ values for chlorophenols were linearly correlated to the Hammett constant and the octanol-water partition coefficient (D'Oliveira et al., 1993). The Hammett constant, σ, is a measure of the electronic effect of benzene ring substituents and whereas the octanol-water partition coefficient, $K_{ow}$, is a commonly used in the environmental studies of organic destruction in aqueous media as a liquid-phase solute descriptor (Pareek, and Adesina 2003).

### *2.1.4 $TiO_2$ semiconductor as a photocatalyst*

According to Pareek and Adesina (2003) $TiO_2$ semiconductor in anatase form has a relatively high energy band gap (3.2 eV), corresponding to beginning irradiation of λ below 387 nm. The rutile form of $TiO_2$ has a slightly smaller energy bandgap (3.02 eV), and the absorption begins at 410 nm. Figure 2.3 shows the various semiconductor energy bandgaps in aqueous electrolyte at pH = 1 (Linsebigler *et al*., 1995). In order to reduce a chemical species, the conductance band of the semiconductor must be more negative than the reduction potential of the chemical species.

On the other hand, the potential of the valence band of the semiconductor must be more positive than the oxidation potential of the chemical species to make the photooxidation of a chemical species happens (Mills *et al*., 1993). However, the anatase form of $TiO_2$ shows much higher photoactivity than the rutile form (Augugliaro *et al*., 1988 and Matthews, 1988) due to a faster recombination of the charge carriers in rutile:

$$e^- + h^+ \rightarrow \text{heat} \quad (2.4)$$

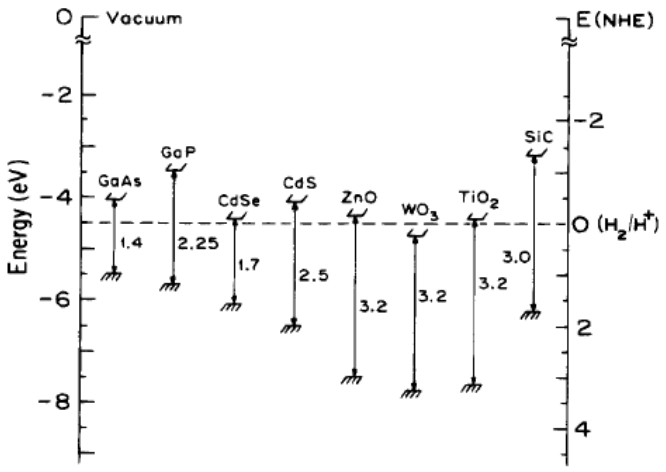


**Figure 2.3** Energy bandgap of various semiconductors (Mills *et al*., 1993)

Also by a considerably lower amount of surface hydroxyl groups leads to fewer reactants adsorbed on the rutile surface. A widely used commercial $TiO_2$ photocatalyst, which is Degussa P 25, consists of 70 – 80 % of anatase form with BET surface area about 50 $m^2g^{-1}$ and particle size around 30 nm. Generally speaking, irradiation with UV light (wavelength below 400 nm) will cause electron excitation to the conduction band of $TiO_2$ semiconductor. This electron excitation leads to holes (positively charged sites) formation in the valence band.

A study using ultrafast laser flash photolysis using colloidal $TiO_2$ showed that the generation of these charge carriers happened within a few femtoseconds ($10^{-15}$ seconds) after the photon absorption (Colombo and Bowman, 1995 & 1996; Colombo *et al*., 1995). After their generation, the photogenerated electron and holes are migrating to the semiconductor surface. In the $TiO_2$ particles normally used in the water treatment photocatalytic degradation, the transfer time was estimated only some ten picoseconds ($10^{-12}$ seconds) (Hufschmidt *et al*., 2004). Furthermore, these surface charge carriers are trapped in the subsurface and surface states of the semiconductor particle, for example: oxygen vacancies in $TiO_2$ may act as electron traps (Hoffmann *et al*., 1995)**.**

$$e_{CB}^- \rightarrow e_{tr}^- \quad (2.5)$$

$$h_{VB}^+ \rightarrow h_{tr}^+ \quad (2.6)$$

Where: $e_{tr}^-$ and $h^+_{tr}$ represent the trapped electron and holes.

The trapping process takes place nearly as fast as the transfer process. Hoffmann *et al*. (1995) proposed a general mechanism for heterogeneous photocatalysis on $TiO_2$, which has several primary processes:

1. charge-carrier generation

$$TiO_2 + h\nu \rightarrow h_{vb}^+ + e_{CB}^- \qquad \text{(femto-seconds)} \qquad (2.7)$$

2. charge-carrier trapping

$$h_{vb}^+ + >Ti^{IV}OH \rightarrow \left[>Ti^{IV}OH\bullet\right]^+ \qquad \text{(fast, 10 ns)} \qquad (2.8)$$

$$e_{cb}^- + >Ti^{IV} \rightarrow \left[>Ti^{IV}OH\right] \qquad \text{(shallow trap, 100 ps, equilibrium)} \qquad (2.9)$$

$$e_{cb}^- + >Ti^{IV} \rightarrow >Ti^{III} \qquad \text{(deep trap, 10 ns, irreversible)} \qquad (2.10)$$

The dynamic equilibrium of the reversible trapping of a conduction-band electron in a shallow trap below the conduction-band edge suggests that there is a limited probability that $e_{tr}^-$ can be transferred back into the conduction band at room temperature.

3. charge-carrier recombination

$$e_{cb}^- + \left[>Ti^{IV}OH\bullet\right]^+ \rightarrow >Ti^{IV}OH \qquad \text{(slow, 100 ns)} \qquad (2.11)$$

$$h_{vb}^+ + \left[>Ti^{IV}OH\bullet\right]^+ \rightarrow >Ti^{IV}OH \qquad \text{(fast, 10 ns)} \qquad (2.12)$$

4. interfacial charge transfer

$$\left[>Ti^{IV}OH\bullet\right]^+ + Red \rightarrow >Ti^{IV}OH + Red\bullet^+ \qquad \text{(slow, 100 ns)} \qquad (2.13)$$

$$e_{tr}^- + Ox \rightarrow >Ti^{IV}OH + Ox\bullet^+ \qquad \text{(very slow, ms)} \qquad (2.14)$$

Where >TiOH represents the primary hydrated surface functionality of $TiO_2$; $e_{cb}^-$ is a conduction-band electron; $e_{tr}^-$ is a trapped conduction-band electron, $h_{vb}^+$ is a valence-band hole; Red is an electron donor (reductant); Ox is an electron acceptor (oxidant); $[>Ti^{IV}OH]^+$ is the surface-trapped VB hole (i.e., surface-bound hydroxyl radical); and $[>Ti^{III}OH]$ is the surface-trapped CB electron.

Therefore, based on the above mechanism, there are two critical processes which determine the overall quantum efficiency for interfacial charge transfer (Hoffmann *et al*., 1995), which are the competition between charge carrier recombination and trapping (picoseconds to nanoseconds) as well as, consecutively, the competition between trapped carrier recombination and interfacial charge transfer (microseconds to milliseconds). Either a delay in the charge carrier recombination or an increasing rate of the interfacial electron-transfer is expected to result in higher quantum efficiencies.

In an n-type semiconductor like $TiO_2$, the reactive species is the hole which carries the major part of the light energy giving a driving force for photo-oxidation of the organic molecules at the surface (Gerishcer and Heller, 1991). Photogenerated holes may react with surface adsorbed water to produce hydroxyl radical $^{\bullet}OH$ (Bickley and Stone, 1973; Turchi and Ollis, 1990).

$$H_2O_{ad} + h^+_s \rightarrow \bullet OH_{ad} + H^+_{ad} \tag{2.15}$$

In the same way, the positive holes can be trapped by surface hydroxyl groups to form the same radical.

$$OH^-_{ad} + h^+_s \rightarrow \bullet OH_{ad} \tag{2.16}$$

$OH^-$ group may be formed by partial hydrolysis of the oxide on the surface or by specific dissociative water adsorption into $OH^-_{ad}$ or $H^+_{ad}$ at different surface sites (Moser and Gratzel, 1982; Salvador, 1981). Many supporting observations obtained through different techniques involve the generation of •OH as an active species (Anpo *et al*., 1985). Thus, this radical is often considered as the principal species for photocatalytic oxidation reactions. However, other recent studies have suggested that oxidation may occur directly via the photogenerated holes (Carraway *et al*., 1994; Ishibashi *et al*., 2000; Mao *et al*., 1991). The rationale of this idea is that the holes possess extremely positive oxidation potential and should thus be able to oxidize almost all chemicals (Bahnemann *et al*., 1991). The oxidizing radicals may be present either in the fluid phase or adsorbed state (Trillas *et al*., 1992). A general mechanism of photodegradation of an organic pollutant has been proposed by Adesina (2004) as follows:

| | | |
|---|---|---|
| $SC + h\nu \rightarrow e_s^- + h_s^+$ | *ion of electrons and holes* | (2.17) |
| $OP(aq) \rightarrow OP^+(aq) + OP^-(aq)$ | *dissociation of organic pollutant* | (2.18) |
| $O_2(dissolved) + e_s^- \rightarrow O_{2s}^-$ | *adsorption of dissolved $O_2$* | (2.19) |
| $OP^-(aq) + h_s^+ \rightarrow OP_s\bullet$ | *production of surface organic radicals* | (2.20) |
| $H_2O + h_s^+ \rightarrow H^+(aq) + OH_s\bullet$ | *photosplitting of water* | (2.21) |
| $H^+(aq) + O_{2s}^- \rightarrow H_2O_{2s}\bullet$ | | (2.22) |
| $OH^- + h_s^+ \rightarrow OH_s\bullet$ | | (2.23) |
| $H_2O_{2s}\bullet + H^+(aq) \rightarrow H_2O_2 + h_s^+$ | | (2.24) |
| $OP_s\bullet + OH_s\bullet/HO_{2s}\bullet \rightarrow M_{nS}\bullet$ + neutral site | | (2.25) |
| $M_{nS}\bullet + OH_s\bullet/HO_{2s}\bullet$ ® ...$CO_2 + H_2O$ + mineral acids | | (2.26) |
| $OP^+(aq) + OH^-(aq) \rightarrow$ hydroxylated products | | (2.27) |
| $e_s^- + h_s^+ \rightarrow SC$ + heat | *degradative electron-hole recombination* | (2.28) |

where SC is the semiconductor; $OP^+$ and $OP^-$ are organic cation and anion, respectively; the subscript s refers to a surface entity; and $M_n$ are intermediates in the reaction path to complete mineralization. In some cases, $OP^+$ may be simply the $H^+$ ion and $OP^-$ is the conjugate base, while in others $OP^+$ may be a metal cation.

### 2.1.5 Photo-oxidation of organic molecules on the $TiO_2$ photocatalyst interface

A wide range of toxic chemicals has been treated by photocatalytic processes to test the general applicability of the method. Halogenated hydrocarbons are readily mineralized in aqueous suspension of $TiO_2$ photocatalyst (Pruden and Ollis, 1983; Nguyen and Ollis, 1984), with general stoichiometry as follows:

$$C_xH_yCl_z + \left(x + \frac{y-z}{4}\right) O_2 \rightarrow xCO_2 + zHCl + \left(\frac{y-z}{2}\right) H_2O \quad (2.29)$$

Aromatic molecules, such as phenol, are also photocatalytically oxidized with following stoichiometry (Okamoto *et al*., 1985):

$$C_6H_5OH + 7\ O_2 \rightarrow 6CO_2 + 3\ H_2O \qquad (2.30)$$

Dyes, phthalates, DDT, and surfactants are other classes of chemicals that can be destroyed by using $TiO_2$ photocatalyst. Table 2.1 lists the different types of organic molecules that have been mineralized with $TiO_2$ – UV photocatalysis (Mills and Hunte, 1997; Herrmann, 1999). The photo-mineralization process typically proceeds through a series of intermediates formation whose O/C ratio is progressively higher and eventually is oxidized into $CO_2$ and $H_2O$ (Serpone, 1996). Successful photocatalytic destruction of some toxic non-biodegradable pesticides and herbicides with assistance of oxidizing agents, such as $H_2O_2$ (hydrogen peroxide) and $S_2O_8^{2-}$ (peroxy-disulphate), have been reported (Malato *et al*., 2000**;** Parra *et al*., 2000). The non-selective and total photooxidation properties of the $TiO_2$ particles in aqueous suspension are related to the strong oxidizing agents (photogenerated holes, OH and peroxide radicals) formed, as previously described, during the photocatalytic process.

**Table 2.1:** Examples of $TiO_2$ – UV photo-mineralization of various organic substrates (Mills and Hunte 1997; Herrmann, 1999)

| Class | Example |
|---|---|
| Alkenes | Methane, isobutane, pentane, heptane, cyclohexane, paraffin |
| Haloalkanes | Mono-, di-, tri-, and tetrachloromethane; tribromoethane; |
| Aliphatic alcohols | Methanol, ethanol, isopropyl alcohol, glucose, sucrose |
| Aliphatic carboxylic | Formic, ethanoic, dimethylethanoic, propanoic, oxalic acids |
| Alkenes | Propene, cyclohexene |
| Haloalkenes | Perchloroethene; 1,2-dichloroethene; 1,l,2-trichloroethene |
| Aromatics | Benzene, naphthalene |
| Haloaromatics | Chlorobenzene; 1,2-dichlorobenzene, bromobenzene |
| Nitrohaloaromatic | 3,4-dichloronitrobenzene |
| Phenols | Phenol, hydroquinone, catechol, 4-methylcatechol, |
| Halophenols | 2-, 3-, 4- chlorophenol; pentachlorophenol; 4-fluorophenol; |
| Aromatic carboxylic | Benzoic, 4-aminobenzoic, phthalic, salicylic, m-and p- |
| Polymers | Polyethylene, polyvinylchloride (PVC) |
| Suffactants | Sodium dodecylsulphate (SDS), polyethylene glycol, |
| Herbicides | Methyl viologen, atrazine, simazine, prometron, propetryne, |
| Pesticides | DDT, parathion, lindane |
| Dyes | Methylene blue, rhodamine B, methyl orange, fluorescein |
| Amides | Benzamide |

## 2.2 Modification Techniques of $TiO_2$ Photocatalyst

Two kinds of imperfection limit the $TiO_2$ photoactivity, namely, its relatively large band gap and recombination of the photogenerated electron-hole pairs (Xu *et al*., 2002). Many workers have investigated various ways to modify the electronic properties of the $TiO_2$ photocatalyst in order to extend the absorption region to visible light as well as to reduce electron-hole recombination rates (Justicia *et al*., 2002). Unfortunately, it is extremely difficult to compare the improvement achieved from study to study.

One approach is to couple $TiO_2$ photocatalyst with other semiconductor photocatalysts, such as $WO_3$ and $In_2O_3$ (Engweiler *et al*., 1996; Poznyak *et al*., 2001). This method can enhance the charge separation of electrons and holes. To extend the absorption region to visible light, two different approaches can be used.

Firstly, by reducing the ratio of oxygen to titania to a number less than two. Simple wet process by calcination of the hydrolysis product of titanium sulfate with ammonia was

used to shift the absorption region in 400 – 550nm (Ihara *et al*., 2003). Another similar attempt by using metal organic chemical vapor deposition resulted in thin film $TiO_2$ photocatalyst with enhanced photoactivity under vis-light range (Justicia *et al*., 2002). Experimental evidence showed that the gap-narrowing induced by the presence of oxygen vacancies is the main factor for the enhanced activity in the visible region.

Secondly, by introducing states within the $TiO_2$ bandgap that absorbs the visible light region. In this strategy, doping metal ions into $TiO_2$ lattice is probably the most widely used technique.

### 2.2.1 Doping various types of metal ions into $TiO_2$

The rationale for doping $TiO_2$ with metal ion is based on three possible benefits, which are band-gap reduction, charge separation in order to minimize the electron-hole recombination rate, and the promotion of active defect sites that function as reactive surface centers (Pareek and Adesina, 2003). Three groups of metal dopants are commonly used for titania modification: alkaline earth metals (such as Li, Ca, and Ba) (Anpo *et al*., 1998), transition metals (for example Co, Cr, Fe, Cu, and Ru) (Iwasaki *et al*., 2000, Sakata *et al*., 1998, Wang *et al*., 2000) and lanthanide or rare earth elements (Eu, La, Nd, and Pr) (Rodrriguez-Talavera *et al*., 1997).

Doping titania with some transitional metal ions can significantly extend the absorption band of the photocatalysts into visible region (Dvoranova *et al*., 2002). In addition, doping selective metal ion such as Bi into $TiO_2$ by using metalorganic decomposition method causes an effective charge separation to inhibit electron-hole recombination (Xu *et al*., 2002) and thus enhance the photoactivity of $TiO_2$ photocatalysts. However, some workers argue that introducing certain metal ions will reduce the activity of the photocatalysts. The doped metal ions can act as recombination centers (Asahi *et al*., 2001; Choi *et al*., 1994; Haber, 1991). As the result, fewer charge carriers will facilitate redox processes onto the photocatalyst surface. In the context of photooxidation process, the ability of the photocatalysts to generate reactive radical species will be reduced.

Therefore, the photoactivity of the doped-$TiO_2$ photocatalysts is determined by the type of dopants ion and its concentration within $TiO_2$ photocatalysts as well as method of preparation used, including associated thermal treatment (Blazkova *et al*., 1998; Litter, 1999; Raphael *et al*., 1989; Wilke and Breuer, 1999; Wong and Malati, 1986). Sol-gel and precipitation preparation methods are commonly used to synthesize oxide supports (Rodríguez *et al*., 1992), such as alumina ($Al_2O_3$) or titania ($TiO_2$). Precipitation method involves the precipitation of the corresponding salt (chloride or nitrate) with ammonium hydroxide to obtain precipitate, which is then dried and calcined.

There are several different routes to synthesize metal-doped titania photocatalysts. Xu *et al*. (2002) used a sol-gel method to prepare rare-earth-doped $TiO_2$ from tetra-n-butyl titanate. Precipitation from titanium sulphate and chloride in ethanol solution was employed by other groups (Dvoranova *et al*., 2002; Iwasaki *et al*., 2000). Tahiri *et al*. (1998) synthesized Cr and Pt doped titania using flame hydrolysis and wetness impregnation method. Among those methods, the sol-gel method offers more homogenous (molecular level) mixing, low calcination temperature, and producing higher surface area. Therefore, the sol-gel method is preferred and then will be described in more details. Moreover, results from previous studies on doping ions of various groups of metals into $TiO_2$ photocatalyst will also be presented.

## 2.3 Visible Light Photocatalysis

Besides the approaches previously discussed in the section 2.2, in order to utilize radiation in the visible spectrum of the sun for $TiO_2$-based photocatalytic reaction purposes, some other approaches had been investigated, namely, dye-modified $TiO_2$ photocatalysts.

## 2.4 General Description of Modified Doped $TiO_2$

Various modification methods, such as metal ion and non-metal co-doping, metal ion absorption or noble metal deposition on the surface of non-metal-doped $TiO_2$, coupling

metal oxides with non-metal-doped $TiO_2$, have been investigated by many researchers, as shown in Tables 2.2, 2.3 and 2.4. In the metal & non-metal codoping, the other dopant is usually a transition metal or rare-earth metal ion. Various metal ions such as $Fe^{3+}$, $Ta^{2+}$, $Ni^{3+}$, $V^{5+}$, $Cr^{3+}$, $W^{5+}$, $Ce^{3+}$, $La^{3+}$ and $Sm^{3+}$ were reported to co-dope $TiO_2$ with non-metal. Non-metal elements, such as F, B, S, C, P and Si have been used to co-dope $TiO_2$ with non-metal. Noble metals, such as Au, Pt, Pd, deposited on metal oxides, such as $V_2O_5$, $WO_3$ and $ZrO_2$, dispersed on the surface of non-metal-doped $TiO_2$ have been investigated.

**Table 2.2** Metal doped $TiO_2$ photocatalysts and the preparation method and the potential application used for testing the photocatalytic activity

| Doped element | Preparation method | Potential application | References |
|---|---|---|---|
| Ag | Silver nitrate was mixed with reduction agent (sodium citrate tribasic dihydrate) and the reaction temperature was raised to 80°C with continuous stirring. Then TIP and $HNO_3$ were added and the reaction was maintained at 50°C for 24 h. The prepared sol was dried at 105°C for 24 h and calcined at 300°C. | Degradation of nitrophenol in aqueous phase | Lee *et al.,* 2005 |
| Fe | The reactive magnetron sputtering method: 99.99% titanium target and 99.9% iron pieces were placed in the reaction chamber and mixture of argon and oxygen was introduced into the chamber during discharging. | Wastewater decolouring | Carneiro *et al.,* 2005 |
| V | Sol-gel method: Solution 1 (vanadylacetylacetonate dissolved in n-butanol) was mixed with solution 2 (acetic acid in titanium butoxide) and hydrolyzed (24 h) by the water generated via the estrification of acetic and butanol. The suspension as dried at 150°C, pulverized and calcined at 400°C for 0, 5 h. | Wastewater decolouring | Wu and Chen., 2004 |
| | $NH_4VO_3$ (99%) dissolved in distilled water with strong stirring at 60$^o$C, the pH was adjusted to 2.5 with $HNO_3$ and $Ti(OC_4H_9)_4$ (98%) (1 drop $s^{-1}$). The sols were aged and dried at 80$^o$C in air, then pulverized to powders and were calcined in air for 5 h at 600$^o$C. The photodegradation was done of methyl orange under 30 W fluorescent lamp ($\lambda$ = 400 – 750nm). | Photodegradation of methyl Orange | Zhou *et al.,* 2010 |
| Au | Titanium (IV) butoxide dissolved in absolute ethanol was added to solution containing tetrachloroauric acid ($HAuCl_4 \cdot 4H_2O$), acetic acid and ethanol. The resulting suspension was aged (2 | Wastewater decolouring | Li *et at.,* 2001 |

| | | | |
|---|---|---|---|
| | days), dried under vacuum, grinding and calcinated at 650°C. | | |
| Pt | Photoreduction process: $TiO_2$ was suspended in a mixture of hexachloroplatinic acid in methanol. The suspension was irradiated with a 125 W mercury lamp (60 min.). Pt-$TiO_2$ was separated by filtration, washed with distilled water and dried at 100°C for 24 h. | Wastewater decolouring | Li *et at.,* 2002 |
| Cu | $TiO_2$ support was impregnated with aqueous $Cu(NO_3)_2.3H_2O$, standing at room temperature for 24 h. Water was evaporated by heating at 373K for 24 h. The dried solids were fired in air at 773K for 24 h. | Photo-oxidation of Organic acids | Paola *et al.,* 2004 |
| $La_2O_3$ | $La_2O_3/TiO_{2-x}F_x$ photocatalysts were prepared by a simple sol-gel process using tetrabutyltitanate (TBT), La(NO3)3 and NH4F as precursors. | Photo-oxidation of 4-chlorophenol | Cao *et al.,* 2010 |

**Table 2.3** Non-metal doped $TiO_2$ photocatalysts and the preparation method and the potential application used for testing the photocatalytic activity

| DOPED ELEMENT | **Preparation method** | **Potential application** | **References** |
|---|---|---|---|
| N | Titanium nitride (TiN) oxidation: Heating of TiN at 450-550°C for 2h in air (heating and cooling temperature rate: 2°C/min). | Photooxidation of Aromatic compounds | Wu *et al.,* 2008 |
| | Treating anatase TiO2 powder ST01 in the $NH_3$ (67%)/Ar atmosphere at 600°C for 3 h. | Photooxidation of acetaldehyde in gasphase | Asahi *et al.,* 2001 |
| S | Oxidation annealing of titanium disulfide ($TiS_2$) at 300-600°C. | Wastewater decolouring | Takeshita *et al.,* 2006 |
| N, S | Hydrolysis of $Ti(SO_4)_2$ in $NH_3$ aqueous solution. Precipitate was centrifuged, washed with distilled water and alcohol. Obtained gels were dried under vacuum at 80 for 10 h and were ground to obtain xerogel. The xerogel was calcinated at 400-800°C in air for 3 h. | Photooxidation of volatile compounds in gas phase (e.g. acetone and formaldehyde | Zhou *et al.,* 2006 |
| C | Sol-gel method: TBOT was hydrolyzed in the presence of ethanol, water and nitric acid; precipitated titanium hydroxide was dried at 110°C and calcinated in air at 150-200°C. | Degradation of NOx; waste water decolouring | Treschev *et al.,* 2008 |
| | Acid-catalyzed sol-gel process. Alkoxidide precursor was dissolved in corresponding alcohol, mixed with hydrochloric acid aqueous solution. Obtained gel was aged for several days and calcinated in air (3 h at 65°C and 3 h at 250°C) and grounded. | Photooxidation of phenol compounds in aqueous phase | Lettmann *et al.,* 2001 |
| B | Anatase $TiO_2$ powder (ST01) was grinding with boric acid triethyl ester and calcinated in air at 450°C. | Photooxidation of phenol compounds in | Zaleska *et al.,* 2007 |

| | | | |
|---|---|---|---|
| | | aqueous phase | |
| P | Sol-gel method: TIP was hydrolyzed in the presence of isopropanol and water, After hydrolysis phosphoric acid was added. Dispersion was stirred for 2h, centrifuged at 3500 rpm and dried at 100°C. Obtained powder was calcinated at 300°C. | Photooxidation ofphenol compounds in aqueous phase | Korosi and Dekany 2006 |

**Table 2.4** Metal and non metal doped $TiO_2$ photocatalysts and the preparation method and the potential application used for testing the photocatalytic activity

| Doped element | Preparation method | Potential Application | Reference |
|---|---|---|---|
| Fe–N | The photocatalyst was prepared by sol–gel method using tetrabutyltitanate, dodecylamine and $Fe(NO_3)_3$ as precursors and calcined at 400 °C for 2 h | Degradation of 1,2,4-dichlorophenol solution | Hao and Zhang 2009 |
| | The photocatalyst was prepared by sol–gel method using tetrabutyltitanate,ammonium chloride and $Fe(NO_3)_3$ as precursors, and heat treated in Teflon lined stainless steel autoclave at 180 °C for 12 h | Degradation of rhodamine B (RB) | Cong *et al.,* 2007 |
| | $Fe^{3+}$ ions were adsorbed on N–$TiO_2$ with redox treatment | Degradation of methylene blue | Xing *et al.,* 2009 |
| V–N | V-Doped $TiO_2$ were prepared through hydrolysis of tetrabutyltitanate in V ion solution, and by nitridation treatment in triethylamine solution | Photodegradation of methylene blue | Gu *et al.,* 2008 |
| Ce–N | The photocatalyst was prepared by sol–gel process using titanium isopropoxide, ammonium nitrate and cerium nitrate as precursors, then heated at high temperature | Degradation of nitrobenzene | Shen *et al.,* 2009 |
| Sm–N | Sm-Doped $TiO_2$ was synthesized by sol–gel process using tetrabutyltitanate and samarium nitrate as precursors, mixed with urea and hydrothermally prepared in the water at 240 °C | Decomposition of 4-chlorophenol | Huang *et al.,* 2009 |
| La–N | La-Doped $TiO_2$ was prepared by co-precipitation using $TiCl_4$ and $LaCl_3$ as precursor, and heated at 500–600 °C in a flow of dry $NH_3$/Ar atmosphere | Degradation of methyl orange aqueous solution | Wei *et al.,* 2004 |
| W–N | W-Doped $TiO_2$ were prepared by the sol–gel method, and then ball-milled with urea | Photo-discolouration methylene blue | Shen *et al.,* 2008 |

| | | | |
|---|---|---|---|
| | The photocatalyst was synthesized by the sol–gel method using $TiCl_4$, $(NH_4)_2WO_4$ and ammonia as precursors | Degradation of phenol | Li *et al.,* 2008 |
| Cr–N | Cr-Doped $TiO_2$ was prepared by sol–gel process using tetrabutyltitanate and $CrCl_3$ as precursors. The photocatalyst was obtained by nitridation through annealing of Cr–$TiO_2$ under ammonia atmosphere | Degradation of MB and M isopropyl alcohol (IPA) | Pan and Wu., 2006 |
| N-F | The photocatalyst was prepared by spray pyrolysis at 700–900 °C using $TiCl_4$ and $NH_4F$ as precursors | Decomposition of acetaldehyde | Li *et al.,* 2005 |
| | The photocatalyst was prepared by sol–gel method using $TiCl_4$, ammonia and $NH_4F$ as precursor, and heated at 100 °C for 4 h | Decolourization of MO solution | Xie and Zhao, 2008 |
| | The photocatalyst was prepared by solvothermal treatment at 160 °C using tetrabutyltitanate, $NH_4F$ and triethylamine as precursors. | Degradation of 4-chlorophenol | Huang *et al.,* 2006 |
| | The photocatalyst was prepared by hydrolysis of titanium isopropoxide with $NH_4F$ aqueous solution, calcined in air at 770 K for 1 h | Degradation of Methylene Blue (MB) | Livraghi *et al.,* 2009 |
| | $TiO_2$ xerogel was treated under supercritical condition in $NH_4F$/EtOH fluid | Degradation of methylene blue | Huo *et al.,* 2009 |
| | The photocatalyst was prepared by hydrolysis of tetrabutyltitanate in an aqueous $NH_4F$ solution, calcined at 500 °C and washed by distilled water to remove impurities | Photoreduction of $Cr^{5+}$ | Wang *et al.,* 2009 |
| B–N | B-Doped $TiO_2$ was prepared by the sol–gel process using $HBO_3$ as boron source; they were then impregnated with guanidine carbonate solution | Degradation of MO | Gombac *et al.,* 2007 |
| Ni–N | The photocatalyst was prepared by sol–gel process using titanium isopropoxide, ammonium carbonate and nickel nitrate as precursors, then heated at high temperature | Degradation of Formaldehyde | Obata *et al.,* 2007 |

| | | | |
|---|---|---|---|
| Ta–N | The photocatalyst was prepared by a radio-frequency (RF) magnetron sputtering method using Ti target with $(Ta_2O_5)_{0.01}(TiO_2)_{0.99}$ pellet in an $Ar/O_2/N_2$ gas mixture | Decomposition of oleic acid | Zhang and Liu 2008 |

# Chapter-3

# MATERIALS AND METHOD

This chapter describes the materials used and methods adopted for carrying out the photocatalytic degradation of the dye.

## 3.1 Materials

### 3.1.1 Dye

Reactive Black 5 was obtained from a small scale dying industry situated in Ludhiana (Punjab). The dye was commercial grade and manufactured by Colorant Pvt. Ltd. India. Its physical chemical data is given in table 3.1:

Table 3.1 Physical-chemical data of Reactive Black 5

| Properties | Typical Value |
|---|---|
| Molecular formula | $C_{26}H_{21}N_5Na_4O_{19}S_6$ |
| Molecular weight | 991.82 |
| Appearance | Dark black powder |
| Dye content | 55% |
| UV adsorption at $\lambda_{max}$ | 597 nm |
| Application | Dyeing of silk, wool, nylon, leather and paper. |

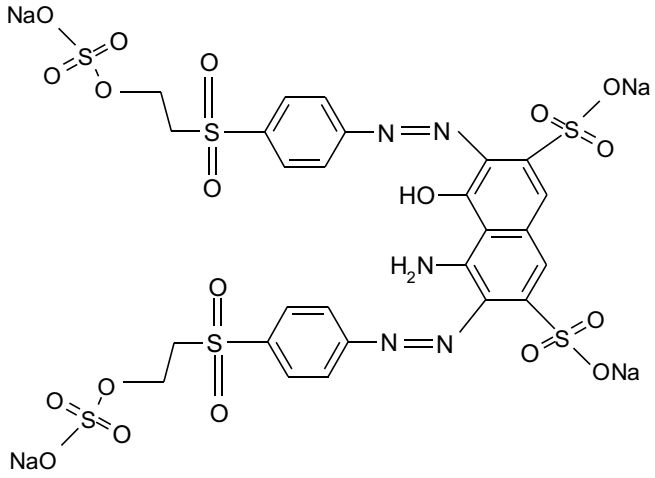


**Figure 3.1:** Molecular structure of Reactive Black 5 dye

### 3.1.2 Catalyst

AEROXIDE® $TiO_2$ P25 was obtained from Evonik Degussa Corporation, USA. Its physico-chemical data is given in table 3.2:

**Table 3.2**: Physico-chemical data of $TiO_2$ P25

| Properties | Units | Typical Value |
|---|---|---|
| Appearance | | Fluffy white powder |
| Specific surface area (BET) | $m^2/g$ | 50±15 |
| Average Particle size | nm | 30 |
| Behaviour towards $H_20$ | | Hydrophilic |
| Crystalline polymorphs | | 70% anatase and 30% rutile |
| Tamped density | $g\ l^{-1}$ | 130 |
| pH in 4% dispersion | | 3.5-4.5 |
| Titanium dioxide content | wt% | ≥ 99.5 |
| HCl Content | wt% | ≤ 0.3 |
| $Al_2O_3$ content | wt% | ≤ 0.3 |
| $Fe_2O_3$ content | wt% | ≤ 0.01 |
| $SiO_2$ content | wt% | ≤ 0.2 |
| Application | | Photocatalytic reaction, raw material, adsorption and thermal stability |

### 3.1.3 Reagents and chemicals

Hydrochloric acid and sodium hydroxide (S. D. Fine Chemicals Limited, India) were used to adjust the pH. $Fe_2(NO_3)_3.10H_2O$ (Lobachemie Limited, India) was used for the doping of $Fe^{3+}$ ions on $TiO_2$. All chemicals were used as received. In all the experiments, distilled water was used for preparing the solutions.

## 3.2 Experimental Setup (UV Chamber and Shallow Pond Reactor)

A schematic diagram of lab scale set up for shallow pond reactor is shown in Figure 3.2. The photocatalytic degradation studies were conducted using Shallow pond slurry reactor. A batch type bench scale photocatalytic reactor system was fabricated for conducting experiments. The set up consisted of a batch reactor placed on a platform under UV light.

A Borosil glass vessel of 500 ml capacity was used as the shallow pond reactor and UV rays were irradiated on the glass vessel. This reactor is placed on a magnetic stirrer to keep the contents in the reactor well mixed, so that the $TiO_2$ remains suspended and the concentration of the pollutant within the reactor could be assumed to be constant at any time. An Eppley radiometer model no. 33013 was used to measure the UV intensity.

**Figure 3.2:** Experimental Setup consisting of UV chamber, magnetic stirrer and slurry pond reactor

## 3.3 Equipment and Instruments

### 3.3.1 Radiometer

The UV light intensity was measured by using an Eppley radiometer (model no. 33013). Its sensitivity is 150 $\mu V/Wm^{-2}$ and response time is milli seconds.

### 3.3.2 Centrifuge

After the photocatalytic treatment of the dye sample, the suspended $TiO_2$ particles have to be separated from the dye sample before measuring its absorbance. The $TiO_2$ particles were separated by using Hitachi High Speed Micro Centrifuge CF15RXII. A centrifuge is a piece of equipment, driven by a motor, which spins liquid samples at high speed (15,000 rpm). The centrifuge works using the sedimentation principle, where the centripetal acceleration is used to separate substances of greater and lesser density.

### 3.3.3 UV-Vis Spectrophotometer

For determining the concentration of various compounds, we first measured the absorbance of the dye sample at $\lambda_{max}$ using UV-Vis spectrophotometer. Then we use calibration curve (concentration versus absorption curve) to determine the concentration of

the dye sample. The concentration of the dye was indirectly determined by measuring absorbance first. For measuring absorbance of the dye samples, Perkin Elmer Lambda 35 UV-Vis spectrophotometer was used.

## 3.4 Experimental Procedures

### 3.4.1 Procedure for photocatalytic experiments using shallow pond slurry reactor under UV light

The general procedure for all the photocatalysis experiments is as follows:

1. The stock solution of Reactive Black 5 dye of concentration 100 mg $L^{-1}$ (100 ppm) was prepared in distilled water for all the experiments.
2. Take 250 ml dye solution from the stock solution in the shallow pond reactor.
3. In the shallow pond reactor, add the desired amount of the $TiO_2$ catalyst.
4. Then check the pH of the solution using Thermo Scientific Orion Star Series Meter.
5. The reactor is placed on the magnetic stirrer and magnetic bead is put in the dye solution for proper stirring.
6. The adsorption of dye on the catalyst is done for 30 minutes in dark condition. An aliquot of 5 ml was taken from the reactor with the help of a syringe. To this 5ml sample of dye, 1:1 dilution is done by adding the equal amount of water. Now, 10 ml solution is poured into centrifuge tube.
7. After 30 minutes, UV lights are switched on. The door of the UV chamber is closed so that no UV rays come out and affect us.
8. After every 30 minutes, take 5 ml sample from the reactor with the help of syringe and 1:1 dilution is done each time.
9. The photocatalysis is done for next 180 minutes.
10. To filter the suspended $TiO_2$ particles from the dye sample, centrifugation is done. Make sure the level of sample in each centrifuge tube is same**.** The centrifuge tubes are spun at the high speed of 15,000 rpm for 15 minutes. The $TiO_2$ particles get settled at the bottom of the tube.
11. A computer based UV-Vis spectrophotometer was used for determination of concentration of samples as per detailed below:
    a. The system is switched on and warmed up.
    b. Thoroughly cleaned quartz cuvettes are taken.
    c. Both cuvettes are filled with distilled water and absorbance at $\lambda_{max}$ (of dye) is checked. Auto zero is done.

**d.** After auto zeroing, one cuvette is filled with the reference compound (distilled water) and the other one with the sample whose absorbance has to be measured at $\lambda_{max}$.

**e.** To get the relationship between concentration and absorbance of the compound, a calibration curve is prepared. Calibration solutions are prepared from standard solutions of known concentration. The absorbance is plotted against known concentration of the calibration samples. These calibration curves are stored in the system itself and the concentration of the unknown sample can be calculated directly from the absorbance.

**12.** Now, we know variation of concentration of dye with time. It decreases with time.

**13.** The conversion percent of RB5 can be obtained in different intervals. The photodegradation efficiency (X) is given by Eq. (3.1)

$$X = \frac{C_0 - C}{C_0} \tag{3.1}$$

**14.** The plot between $\ln(C_0/C)$ and time is plotted and value of rate constant is found.

For degradation of dye with the above mentioned setup, the various experiments were conducted for optimizing the parameters like initial concentration, pH and catalyst loading.

- The dye solution of different concentrations can be prepared by mixing different volumes of dye and distilled water. For example, to make 250 ml dye solution of 50 ppm from stock solution of concentration 100 ppm we mix 125 ml (100 ppm) solution and diluted to 250 ml solution with distilled water. So by this method, we can make dye solution of different concentration like 25 ppm, 50 ppm, 75 ppm, 100 ppm, 125 ppm and 150 ppm etc.
- The pH of the solution (2, 4, 6, 7, 8, and 10) is adjusted by adding HCl or NaOH.

### 3.4.2 Preparation and characterization of $Fe^{3+}$ ion doped $TiO_2$ nanoparticles using wet impregnation method

#### *3.4.2.1 Preparation of $Fe^{3+}$ doped $TiO_2$*

In the wet impregnation method ferric ion ($Fe^{3+}$) doped on $TiO_2$ was prepared according to the following steps. First, 3 g of $TiO_2$ was added to 100 ml distilled water. Then molal

solution of $Fe_2(NO_3)_3.10H_2O$ was prepared. The required amount of $Fe_2(NO_3)_3.10H_2O$ solution for doping was added to $TiO_2$ suspension, where the ferric concentration was 2.0, 4.0 and 6.0 (wt %) of $TiO_2$. The slurry was stirred well and allowed to rest for 24 hrs and then it was washed two times with distilled water to remove undoped metal ions and dried in an air oven at $100^OC$ for 12 h. The dried solids were ground in an agate and mortar and calcined at $500^OC$ for 6 h in a muffle furnace (Behnajady et al., 2008).

#### *3.4.2.2 Characterization of $Fe^{3+}$ doped $TiO_2$*

The XRD technique was used to study crystalline phase to identify and confirm structure of titanium dioxide samples. The XRD spectra of undoped and trivalent ion ($Fe^{3+}$) doped titanium dioxide were obtained with Panalytical X'pert PRO diffractometer over the range of $2\theta$ = 20-80° at room temperature. The external morphology of all $TiO_2$ samples were observed on a SEM: JEOL JSM-6510 LV scanning electron microscope (SEM).

### 3.4.3 Procedure for photocatalytic experiments using shallow pond slurry reactor under visible light

The general procedure is followed for all the photocatalysis experiments as discussed in section 3.5.1. In these experiments the photodegradation was carried out under visible light in place of UV light.

### 3.4.4 Determination of RB 5 concentration

At each stage of photocatalytic degradation, we need to find the concentration of dye. But we can't find the concentration of dye directly so we find absorbance of the dye first. To get the relationship between concentration and absorbance of the compound, a calibration curve is made. Calibration solutions are made from standard solutions of known concentration. We use UV-Vis spectrophotometer to find the absorbance of dye at $\lambda_{max}$. From the graph between concentration and absorbance, we find the concentration of dye at any particular absorbance. The curve between and Concentration and Absorbance is shown in Figure 3.8.

The absorbance obtained at 597 nm for different initial dye concentrations is tabulated in Table 3.3 and these results plotted in Figure 3.8. From the calibration curve of RB 5 (Figure 3.3), we can find the relation between concentration and absorbance.

Concentration = 56.18 X Absorbance (3.1)

So, now we can find the absorbance of dye and by using equation 3.1, we can convert absorbance into concentration of dye.

**Table 3.3**: Variation of absorbance of dye at 597 nm with different concentration of dye

| Concentration (ppm) | Absorbance at 597 nm | Concentration (ppm) | Absorbance at 597 nm |
|---|---|---|---|
| 0 | 0 | 80 | 1.458 |
| 10 | 0.18 | 90 | 1.629 |
| 20 | 0.339 | 100 | 1.821 |
| 30 | 0.502 | 110 | 1.959 |
| 40 | 0.8 | 120 | 2.136 |
| 50 | 1.002 | 130 | 2.304 |
| 60 | 1.143 | 140 | 2.424 |
| 70 | 1.332 | 150 | 2.589 |

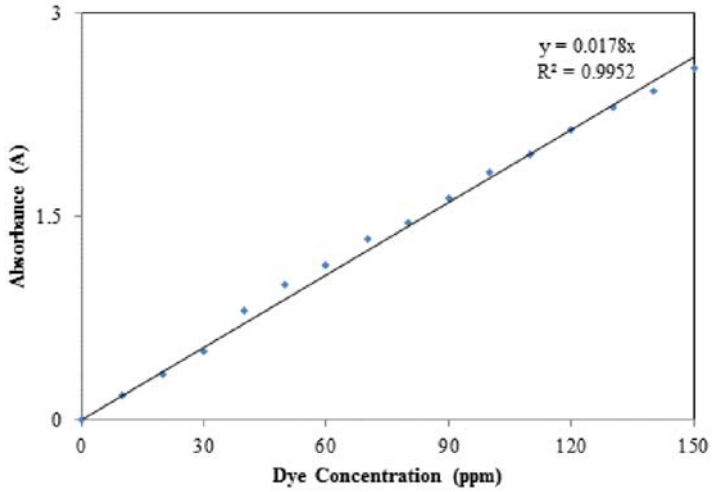


**Figure 3.3:** Calibration curve RB 5 dye at 597 nm

# Chapter-4

# RESULTS AND DISCUSION

Results of analysis of the wastewater from the textile dye using heterogeneous AOP are presented here. This chapter describes three sections. In the first section, the dye effluent was treated with $TiO_2$ and UV light, second section consists of the characteristics of $Fe^{3+}$ ion doped $TiO_2$ using XRD and SEM-EDS. This doped $TiO_2$ was used in the third section for the treatment of RB5 dye using visible light.

**UV-Vis spectral changes**

The changes in the absorption spectra of RB 5 solution during the photocatalytic process at different irradiation times are shown in the Figure 4.1. The spectrum of RB5 in the visible region exhibits a main band with a maximum at 597 nm. The decrease of absorption peaks of RB 5 at $\lambda_{max}$= 597 nm in this figure indicates a rapid degradation of azo dye.

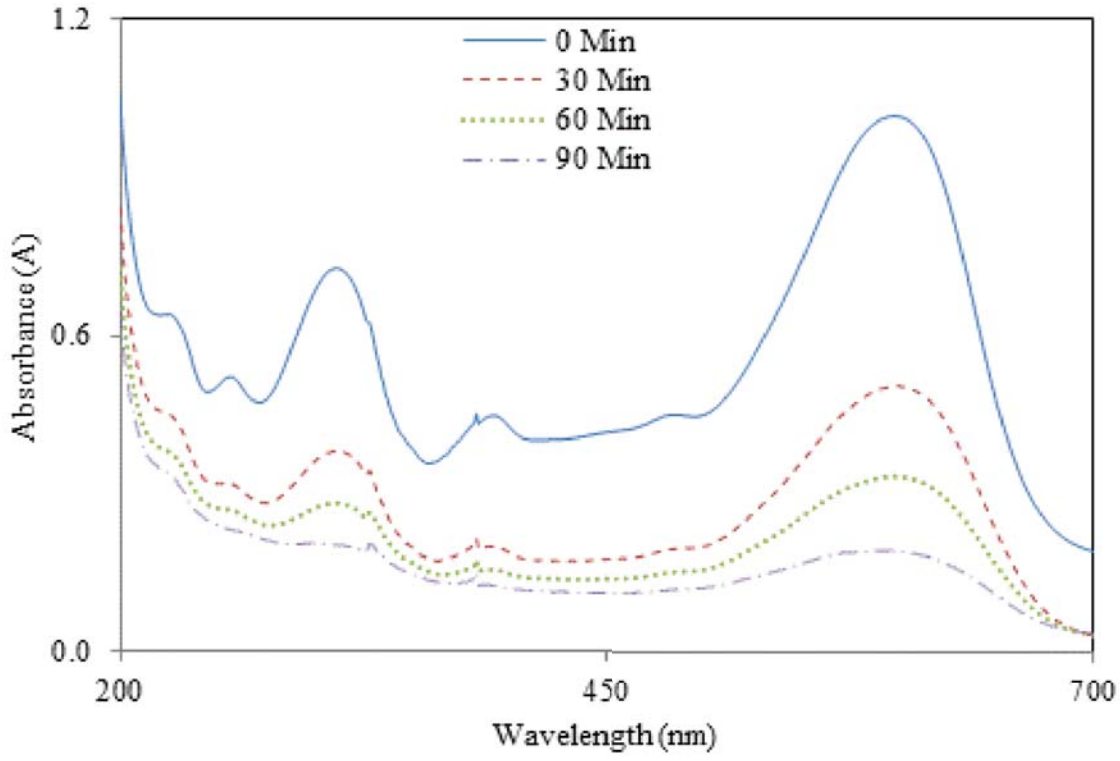


**Figure 4.1:** UV-Vis spectral changes of RB-5 (50 ppm) in aqueous $TiO_2$ dispersion ($TiO_2$ 1 $gl^{-1}$) irradiated with a mercury lamp light at neutral pH, after (1) zero (2) 0.5 h (3) 1.0 h (4) 1.5 h

The decrease is also meaningful with respect to the nitrogen to nitrogen double bond (–N=N–) of the azo dye, as the most active site for oxidative attack.

## 4.1 Photocatalytic Degradation of RB5 in Presence of $TiO_2$ & UV Light

### 4.1.1 Effect of UV irradiation and $TiO_2$ particles

Figure 4.2 shows the effect of UV irradiation and $TiO_2$ particles on photodegradation of RB 5. It can be seen from the figure that in the presence of both $TiO_2$ and UV light, 98.0% of dye was degraded at the irradiation time of 2.5 h. This was compared with 14.0% degradation for the same experiment performed in the absence of $TiO_2$, and the negligible 3 % when the UV lamp had been switched off and the reaction was allowed to occur in the darkness.

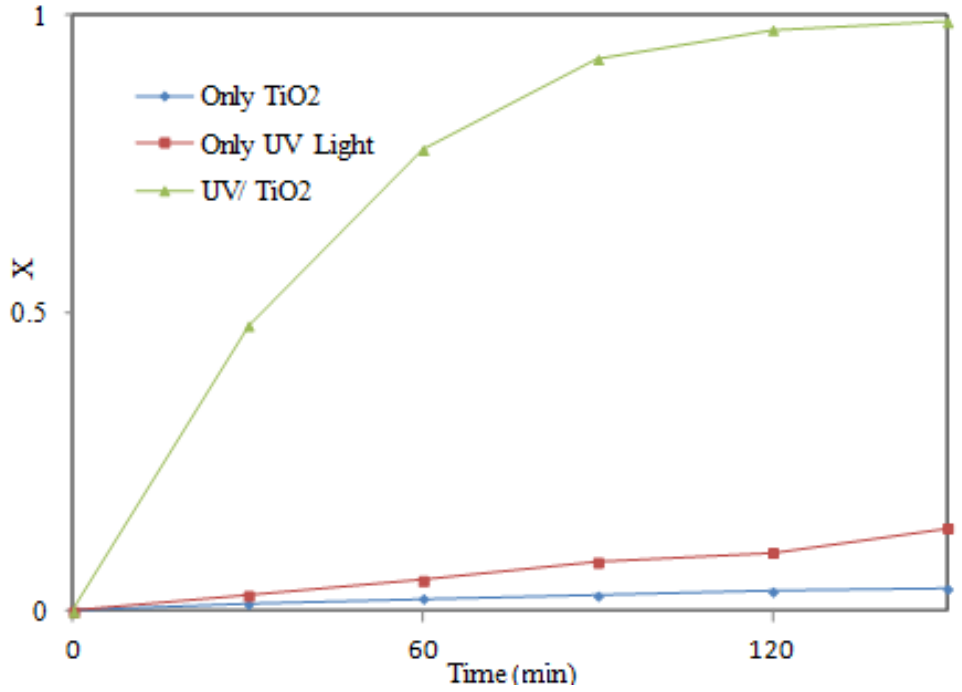


**Figure 4.2:** Effect of UV light and $TiO_2$ on photocatalytic degradation of Co = 50 ppm, $TiO_2$ = 1 $gl^{-1}$, pH = 4

These results show that both UV light and $TiO_2$ are needed for the effective degradation of RB 5. This is due to the fact that when $TiO_2$ is illuminated with the light of $\lambda$ <390 nm, electrons are promoted from the valence band to the conduction band of the semiconducting oxide to give electron–hole pairs. The valence band ($h^+_{VB}$) potential is positive enough to generate hydroxyl radicals at the surface and the conduction band ($e^-_{CB}$) potential is negative enough to reduce molecular oxygen. The hydroxyl radical is a powerful oxidizing agent and attacks organic pollutants present at or near the surface of

$TiO_2$. It causes photooxidation of pollutants according to the following reactions (Eq. 4.1 – 4. 6) (Hoffmann *et al.,* 1995, Fujishima *et al.,* 2000, Galindo *et al.,* 2000).

$$TiO_2 + h\upsilon(\lambda < 390nm) \rightarrow TiO_2(e^-_{CB} + h^+_{VB}) \quad (4.1)$$

$$h^+_{VB} + H_2O_{(ads)} \rightarrow H^+ + OH\bullet_{(ads)} \quad (4.2)$$

$$h^+_{VB} + OH^-_{(ads)} \rightarrow {}^{\bullet}OH_{(ads)} \quad (4.3)$$

$$e^-_{CB} + O2(ads) \rightarrow {}^{\bullet}O^-_{2\,(ads)} \quad (4.4)$$

$$OH\bullet_{(ads)} + dye \rightarrow \text{degradation of the dye} \quad (4.5)$$

$$h^+_{VB} + dye \rightarrow \text{degradation of the dye} \quad (4.6)$$

### 4.1.2 Effect of $TiO_2$ photocatalyst concentration

The photocatalytic degradation of the azo dye (100 ppm) with different $TiO_2$ amounts (0.25, 0.50, 0.75, 1.0, 1.25 and 1.50 $gl^{-1}$) were studied and the obtained results are shown in Figure 4.3. The efficiency of photocatalytic degradation of the dye clearly increased with the increase of the amount of photocatalyst. The efficiency of photocatalytic degradation of 1.5 $gl^{-1}$ of $TiO_2$ degraded around 0.94 of RB 5 in 180 min. However, the efficiency of photocatalytic degradation of 1.0 and 1.25 $gl^{-1}$ of $TiO_2$ in the end of 180 min of irradiation yielded a similar degradation to that of the highest concentration of $TiO_2$ used. This can be explained in terms of availability of active sites on the $TiO_2$ surface and of the light penetration of photo-activating light into the dye-$TiO_2$ suspension; so the effect of the increase on the amount of photocatalyst becomes reduced. For the azo dye studied in this work, the treatment with $TiO_2$ under artificial irradiation of a 250 W mercury vapor lamp was an extremely efficient photodegradation method, since after 2.5 hours dye showed substantial color loss.

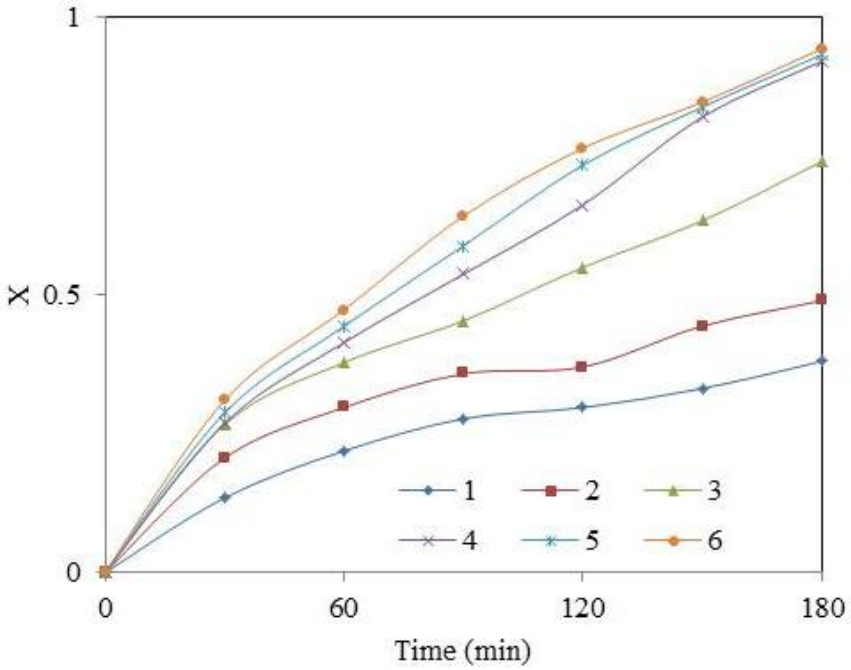


**Figure 4.3:** Effect of the amount of $TiO_2$ on photodegradation efficiency of RB5, Co = 100 ppm, pH = 7. (1) $TiO_2$ = 0.25 $gl^{-1}$ (2) $TiO_2$ = 0.50 $gl^{-1}$ (3) $TiO_2$ = 0.75 $gl^{-1}$ (4) $TiO_2$ = 1.00 $gl^{-1}$ (5) $TiO_2$ = 1.25 $gl^{-1}$ (6) $TiO_2$ = 1.50 $gl^{-1}$

### 4.1.3 Effect of dye concentration

The effect of the initial concentration of RB5 on the decomposition of the dye under the 250 W mercury lamp reactor was determined. The obtained results are presented in Figure 4.4. The results indicate that the decomposition rate of dye strongly depends on the initial dye concentration. The efficiency of photodegradation of both dyes decreased with increase of the initial dye concentration. RB 5 with 25 ppm and 50 ppm of photocatalyst show rates of degradation of 98 and 97 %. On increasing the concentration of the dye until 150 ppm the photodegradation became very slow, presenting a degradation of only 57% for RB 5.

As the initial concentration of the dye increased, more dye molecules were adsorbed on the surface on the catalyst, consequently the generation of hydroxyl radicals was reduced since the active sites were occupied by dyes (Alaton *et al.,* 2001, Daneshvar *et al.,* 2003, Grzechulska and Morawski, 2002). An increase of the initial dye concentration results in an increase of the amount of dye adsorbed on the catalyst surface, affecting the catalytic

activity of the photocatalyst (Carter *et al.,* 2000, Malato *et al.,* 1998). Moreover the reduction of the light path length as the concentration and deepness of the colour of the solution rises also cannot be neglected.

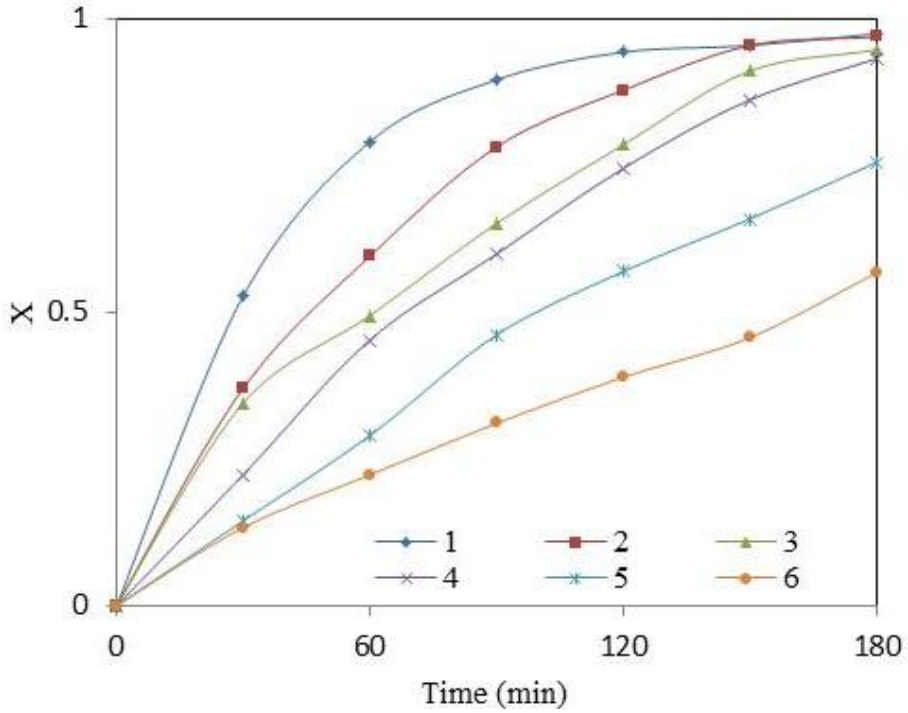


**Figure 4.4:** Effect of initial RB 5concentration on photodegradation efficiency $TiO_2$= 1 $gl^{-1}$ and pH = 7 (1) Co = 25 ppm (2) Co = 50 ppm, (3) Co = 75 ppm, (4) Co = 100 ppm, (5) Co = 125 ppm, (6) Co = 150 ppm

### 4.1.4 Effect of pH

pH is an important parameter for reactions taking place on the surface of a particulate, as is the case of $TiO_2$ photocatalysis. pH variation can in fact manipulate the adsorption of dye molecules onto the $TiO_2$ surfaces (Wang et al., 2008). The effect of solution pH was studied in the range of 2 to 10 for the optimized catalyst amounts (*i.e.*, 1 $gl^{-1}$) and UV-irradiation times (up to 180 min) for the azo dyes under study. Figure 4.5 shows the variation on the efficiency of photocatalytic degradation of RB 5 at different pH values. Photodegradation was higher in acidic media pH 2, 4 and 6 with degradation rates of 99, 98 and 95%, respectively. Up to a pH value of 8, the dye degradation efficiency decreased to 72%. Above pH 7, the degradation continued to decrease to about 51% at pH 10.

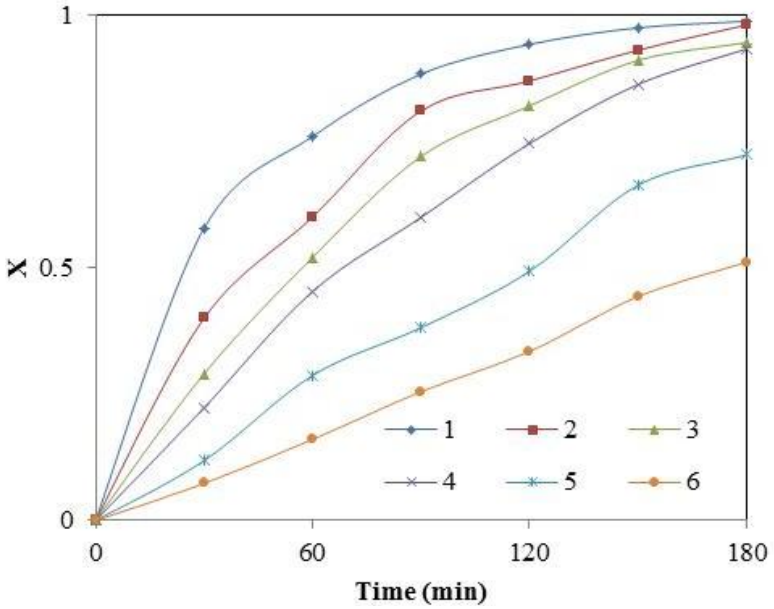


**Figure 4.5:** Effect of pH on photodegradation efficiency of RB 5 at the irradiation time of 3 h. Co = 100 ppm, $TiO_2$= 1 $gl^{-1}$ (1) pH = 2, (2) pH = 4, (3) pH = 6, (4) pH = 7, (5) pH = 8, (6) pH = 10

This catalyst behavior can be explained by $TiO_2$ surface charge density. The point of zero charge of the $TiO_2$ (Degussa P25) is at pH 6.8. In acid media (pH ≤ 6.8) the $TiO_2$ surface is positively charged, whereas under alkaline conditions (pH ≥ 6.8) it is negatively charged (Muruganandham *et al.,* 2006, Dostanic *et al.,* 2011). Considering the structure of RB 5, a positive charge excess in the $TiO_2$ surface promotes a strong interaction with $SO_3^-$ groups of the dye (Figure 4.6 a). A negative charge excess promotes the repulsion of the dye by the titanium surface, diminishing the catalytic activity of this semiconductor (Figure 4.6 b). These results suggest that the influence of the initial pH of the solution on photocatalysis kinetics is due to the amount of the dye adsorbed on $TiO_2$ (Zielinska *et al.,* 2001, Wang *et al.,* 2008). This hypothesis agrees with a reaction occurring at $TiO_2$ surface and not in the solution, close to the surface.

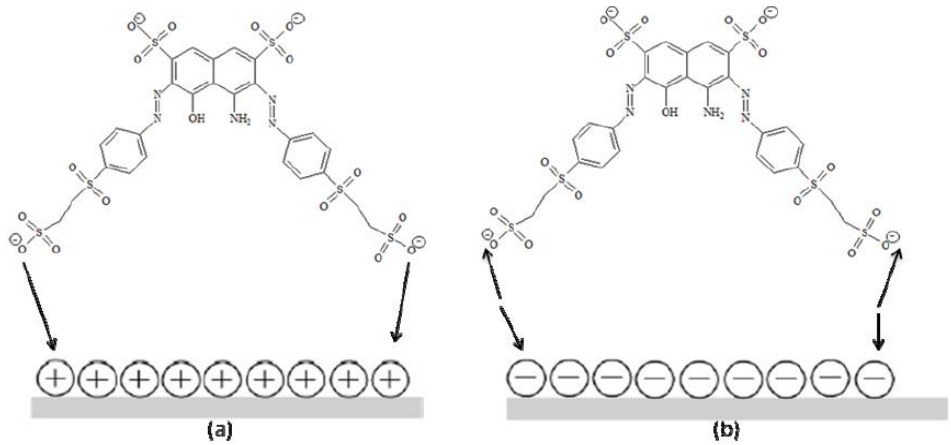


**Figure 4.6:** Schematic interaction model of RB5 and $TiO_2$: (a) acid sites and (b) basic sites (Saggioro *et al.,* 2011)

### 4.1.5 Effect of dye concentration on optimized conditions (pH = 6 and $TiO_2$ loading = 1 $gl^{-1}$)

The effect of dye concentration on optimized conditions (pH = 6 and $TiO_2$ = 1 $gl^{-1}$) was carried out as discussed in section 4.1.3.

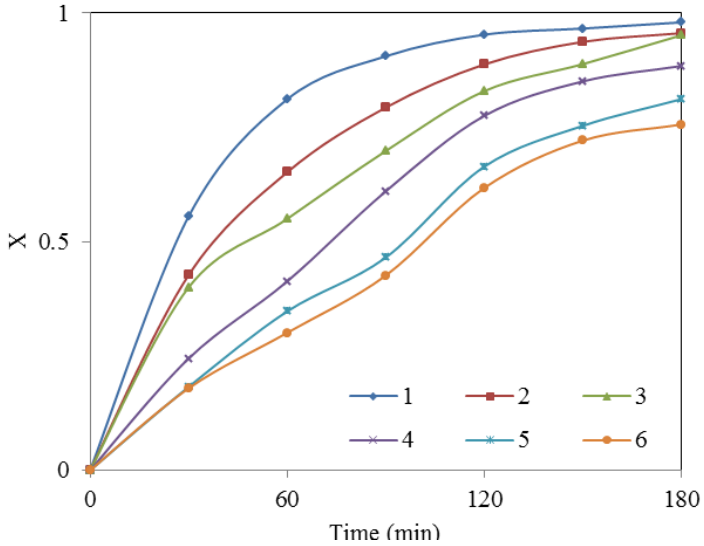


**Figure 4.7:** Effect of initial RB 5 concentration on photodegradation efficiency $TiO_2$= 1 $gl^{-1}$ and pH = 7 (1) Co = 25 ppm (2) Co = 50 ppm, (3) Co = 75 ppm, (4) Co = 100 ppm, (5) Co = 125 ppm, (6) Co = 150 ppm.

### 4.1.6 Kinetics of photocatalytic degradation of RB 5

The plot –ln(C/Co) versus irradiation time for RB 5 was almost linear suggesting that the photodegradation reaction approximately follows the first order kinetics (Figure 4.8).

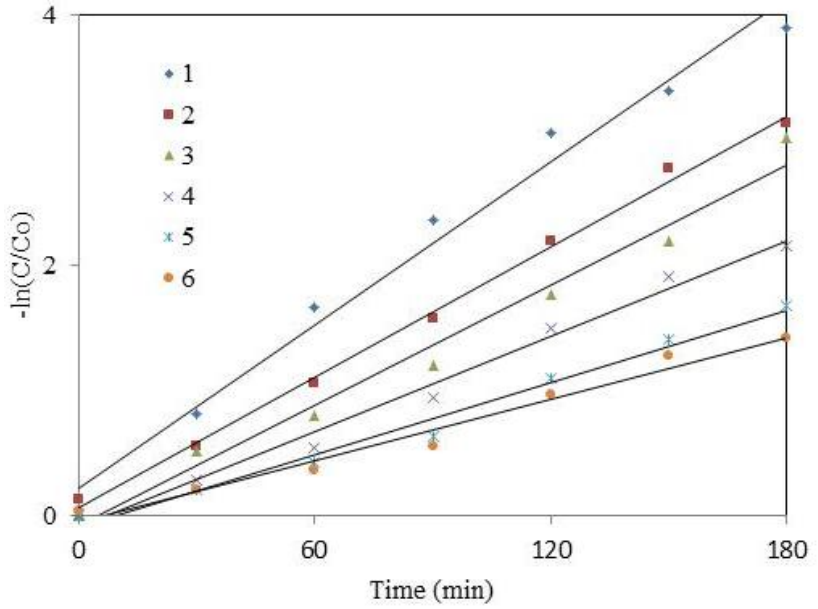


**Figure 4.8:** Reaction kinetics various RB 5 initial concentration and $TiO_2$= 100 $gl^{-1}$, pH = 4. (1) RB 5 = 25 ppm (k = 0.0217 $min^{-1}$), (2) RB 5 = 50 ppm ( k = 0.0173 $min^{-1}$), (3) RB 5 = 75 ppm ( k = 0.016 $min^{-1}$), (4) RB 5 = 100 ppm, ( k = 0.0127 $min^{-1}$), (5) RB 5 = 125 ppm (k = 0.0096 $min^{-1}$), (6) RB 5 = 150 ppm (k = 0.0082 $min^{-1}$).

Rate constants are k = 0.0217 $min^{-1}$ for Co = 25 ppm, k = 0.0173 $min^{-1}$ for Co = 50 ppm, k = 0.0160 $min^{-1}$ for Co = 75 ppm, k = 0.0127 $min^{-1}$ for Co = 100 ppm, k = 0.0096 $min^{-1}$ for Co = 125 ppm, k = 0.0082 $min^{-1}$ for Co = 150 ppm. These were estimated from the slope of the –ln(C/Co) versus time plot in the optimized conditions. The equations and the values of $R^2$ are shown in Table 4.1.

**Table 4.1:** Equations and value of $R^2$ for Reaction Kinetics of RB 5

| Co (ppm) | Equation | $R^2$ |
|---|---|---|
| 25 | y = 0.0217 x + 0.2136 | 0.9819 |
| 50 | y = 0.0173 x + 0.0674 | 0.9968 |
| 75 | y = 0.0160 x + 0.0801 | 0.9813 |
| 100 | y = 0.0127 x + 0.0998 | 0.9875 |
| 125 | y = 0.0096 x + 0.0882 | 0.9834 |
| 150 | y = 0.0082 x + 0.0516 | 0.9752 |

### 4.1.7 Reuse of $TiO_2$ catalyst

The main industrial wastewater treatment approaches are dedicated for the advancement of technologies for environmental benefit. In this study, reuse $TiO_2$ can be predicted as a well exercise for wastewater treatment. Thus, it is required to show that the catalyst can be used

again and again (many times) a significant photocatalyst activity. The $TiO_2$ catalyst was used and recycled for reuse on the Reactive Black 5 degradation; the process was repeated up to six times. The $TiO_2$ recycling studies were performed with 1 $gl^{-1}$ of the catalyst and the efficiency of the photodegradation process was calculated and related between the reuse cycles, as shown in Figure 4.9.

The studies show that $TiO_2$ demonstrated noble permanence after recovery and that catalyst reuse is active. The first cycle degraded 95% of the dye after 180 minutes of irradiation. Subsequently, the second and third cycle degraded 87 and 80% the dye, respectively. After these repetitions, the efficiency evidently decreased, as demonstrated in the fourth, fifth and sixth repetitions, where the rates of degradation decrease to 75, 69 and 63% respectively. Though, the rate of degradation is still substantial after five times of $TiO_2$ reuse. Agglomeration and sedimentation of the dye around $TiO_2$ particles after each cycle of photocatalytic degradation is a possible cause of the observed decrease on the degradation rate, because each time the photocatalyst is reused new parts of the catalyst surface become unavailable for dye adsorption and thus photon absorption, reducing the efficiency of the catalytic reaction.

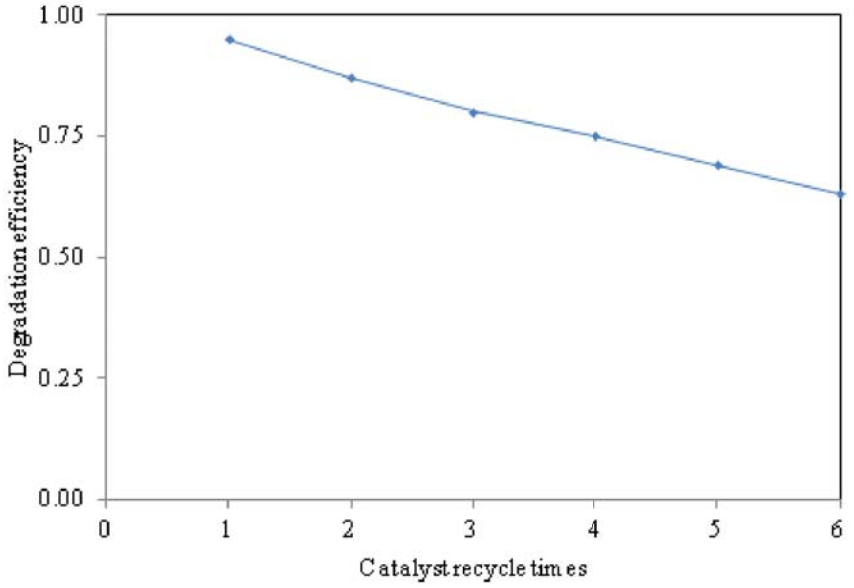


**Figure 4.9:** Effect of reuse of $TiO_2$ catalyst on photodegradation efficiency ($TiO_2$ = 1 $gl^{-1}$, RB 5 = 100 ppm)

## 4.2 Characterization of $Fe^{3+}$ Doped $TiO_2$ Nanoparticles

$TiO_2$ doped with $Fe^{3+}$ designated as Fe-$TiO_2$ was prepared by wetness impregnation processes, using aqueous solution of $Fe_2(NO_3)_3.10H_2O$ as the dopant source. The photograph of blank, 2 % Fe, 4 % Fe and 6 % Fe doped $TiO_2$ powder is shown in Fig 4.10.

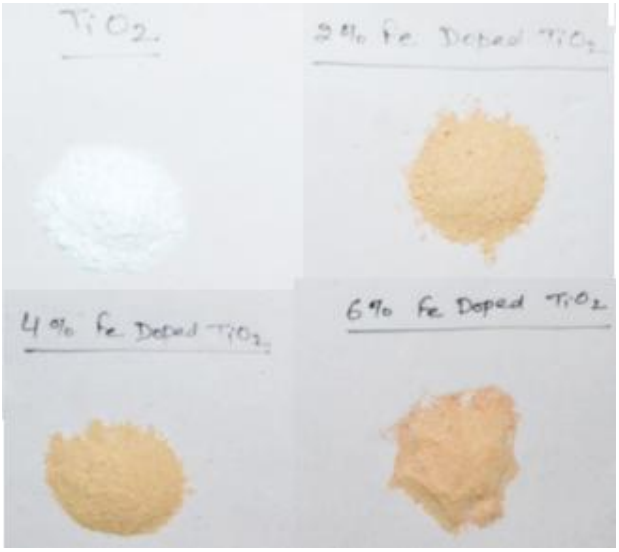


**Figure 4.10:** The photographs of undoped and doped $TiO_2$ powder

### 4.2.1 X-ray powder diffraction (XRD)

XRD measurements were carried out with the Panalytical X'pert PRO diffractometer over the range of 2θ = 20-80° at room temperature and compared with the original commercial $TiO_2$ powders. The identification of a species from its powder diffraction pattern is based upon the position of the lines (in terms of 2θ) and their relative intensities. XRD patterns of commercial $TiO_2$ samples areshown in Fig 4.10. Fig 4.11 (a) shows pattern of both anatase (2θ = 25.4°) and rutile (2θ = 27.5°) phases, Figure 4.11 (b)-(d), show only anatase phase, 2θ = 25.4° and very less rutile (2θ = 27.5°) phase, of $TiO_2$ in the samples.

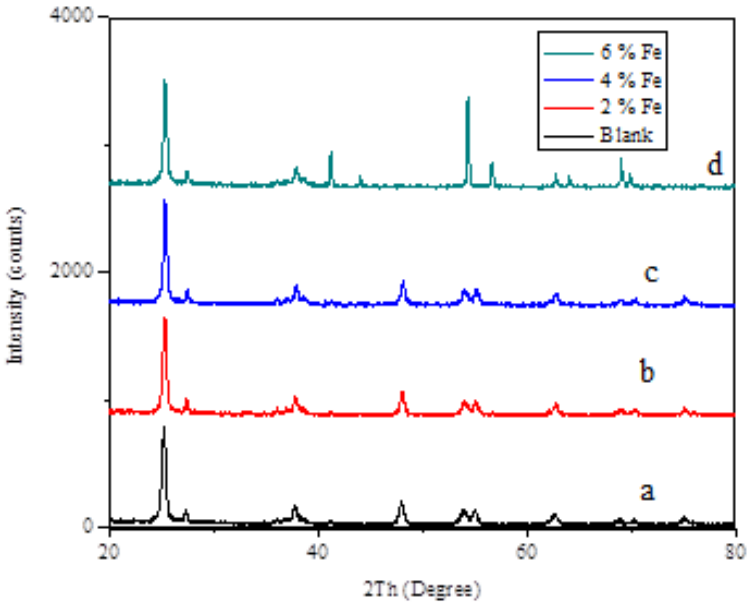


**Figure 4.11:** X-ray diffraction patterns for (a) undoped $TiO_2$, (b) 0.02 Fe-$TiO_2$, (c) 0.04 Fe-$TiO_2$, (d) 0.06 Fe-$TiO_2$

### 4.2.2 Scanning electron microscopy (SEM) and SEM-EDS

SEM is a type of electron microscope that images the sample surface by scanning it with a high-energy beam of electrons in a scan pattern. This technique was used to investigate the surface morphology of $TiO_2$ samples, undoped and doped$TiO_2$. In this work, SEM images were carried out by SEI mode with 20-25 kV. The SEM images of undoped $TiO_2$, doped $TiO_2$ (Fe-$TiO_2$), powders are shown in Figure 4.12-4.13, respectively.

(a) Undoped $TiO_2$ x 200 (b) Undoped $TiO_2$ x 2,000

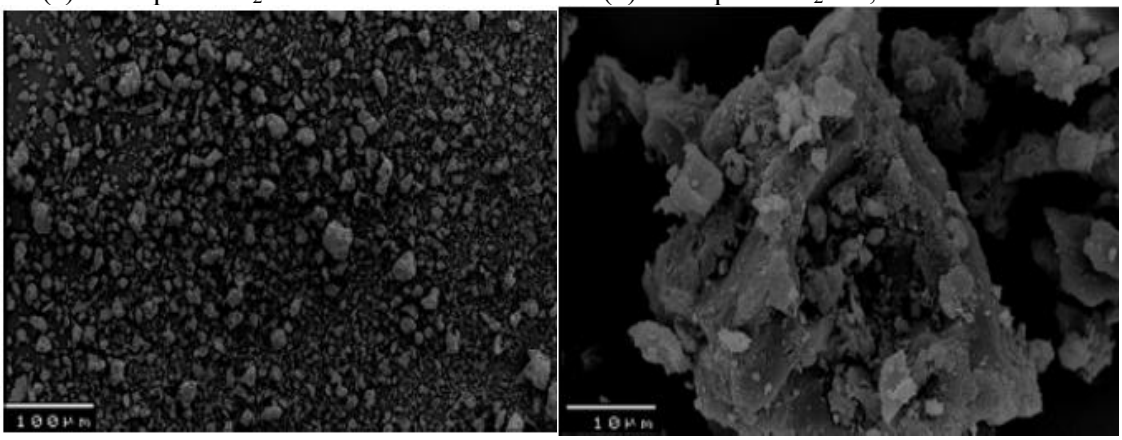

**Figure 4.12:** SEM images of undoped $TiO_2$.

(a) 0.02 Fe-$TiO_2$ x 1000 (b) 0.02 Fe-$TiO_2$ x 3000

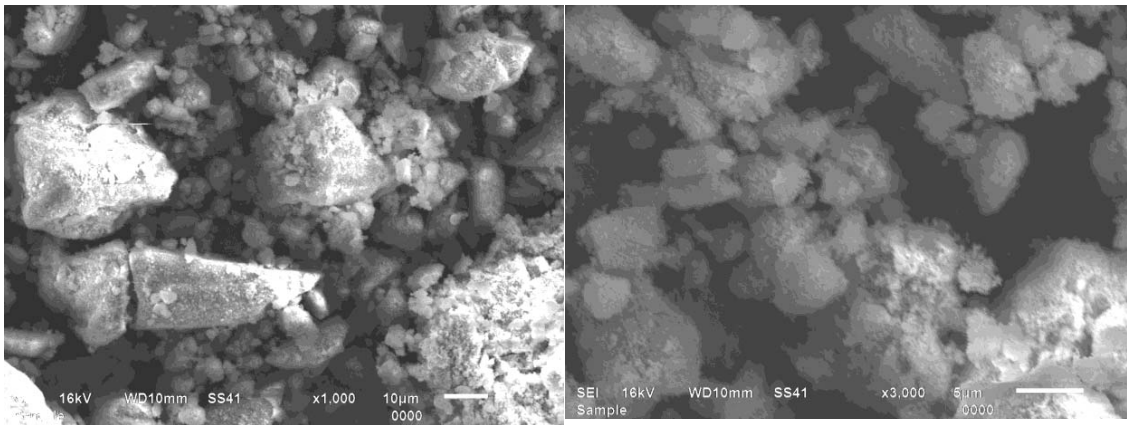


(c) 0.04 Fe-$TiO_2$ x 1000 (d) 0.04 Fe-$TiO_2$ x 3000

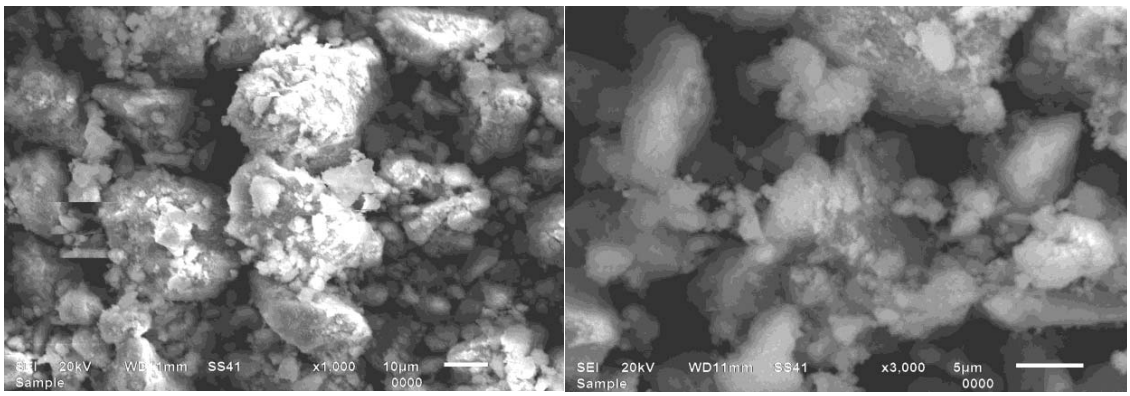


(e) 0.06 Fe-$TiO_2$ x 1000 (f) 0.06 Fe-$TiO_2$ x 3000

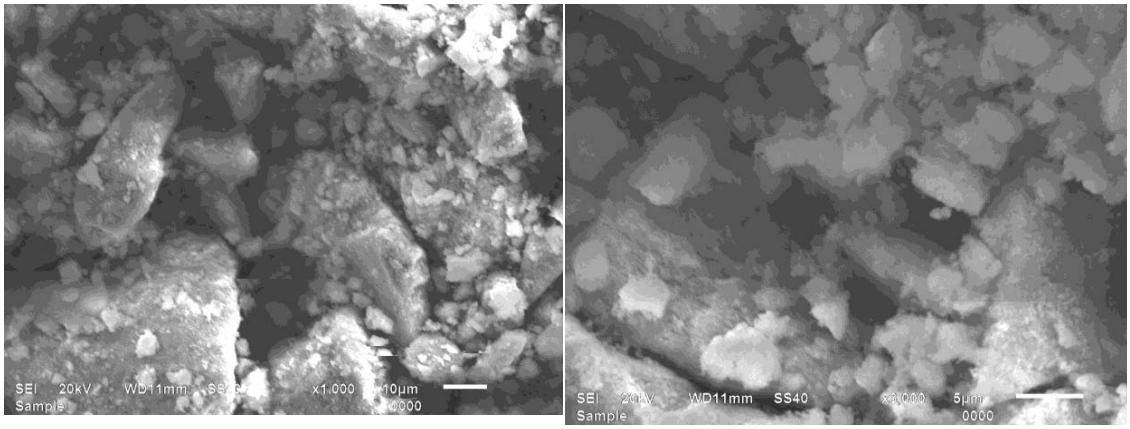


**Figure 4.13:** SEM images of $Fe^{3+}$ ions doped $TiO_2$

The EDS spectra of $Fe^{3+}$ doped $TiO_2$ are shown in Figure 4.14, and the elements content are shown in Table 4.2. It is clearly shown that $Fe^{3+}$ was well dispersed in the $TiO_2$ particles. The calculated $Fe^{3+}$content in the $TiO_2$ particle was 1.86, 3.75 and 5.37 at weight %, which agreed well with the designed doping concentration.

(a) 0.02 Fe-$TiO_2$

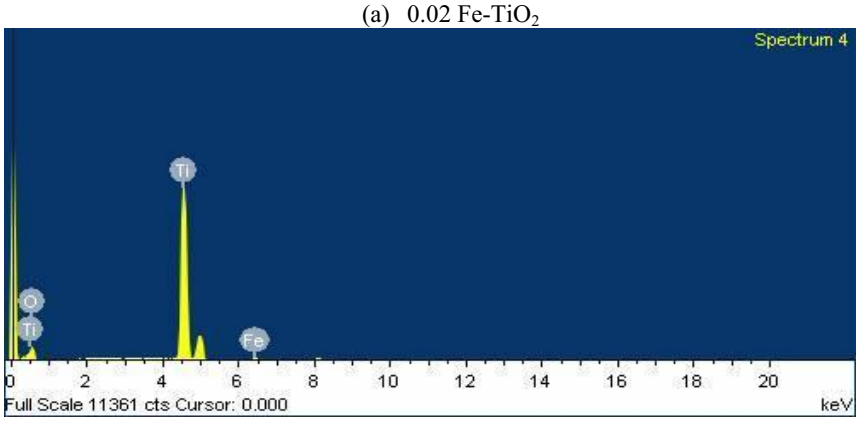


(b) 0.04 Fe-$TiO_2$

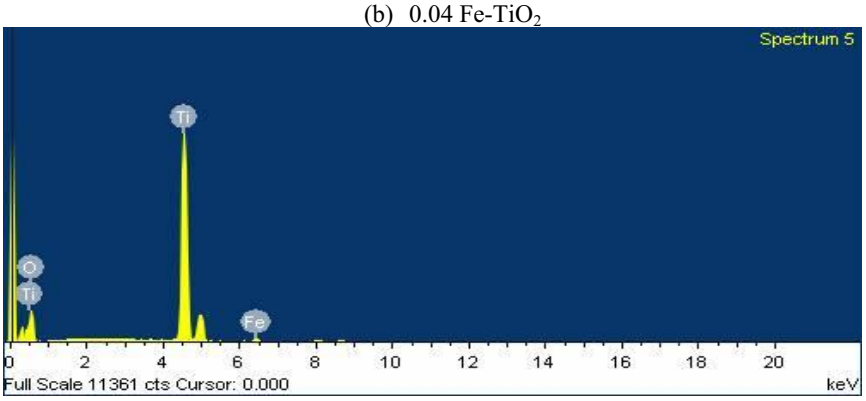


(c) 0.06 Fe-$TiO_2$

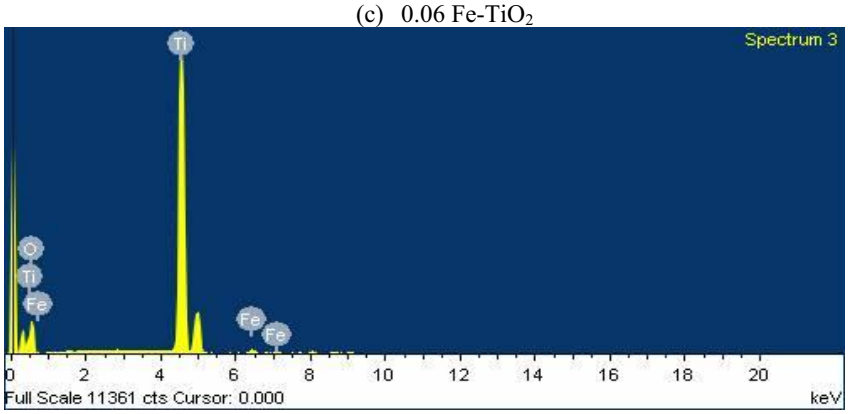


**Figure 4.14:** EDS spectra of $Fe^{3+}$ doped $TiO_2$ particles.

**Table 4.2:** Element content of EDS

| Element | Weight percentage | | |
|---|---|---|---|
| | **0.02 Fe-$TiO_2$** | **0.04 Fe-$TiO_2$** | **0.06 Fe-$TiO_2$** |
| O | 31.06 | 30.2 | 29.58 |
| Ti | 67.08 | 66.05 | 65.05 |
| Fe | 1.86 | 3.75 | 5.37 |
| Total | 100.00 | 100.00 | 100.00 |

## 4.3 Results for Photocatalytic Degradation of RB5 in Presence of $Fe^{3+}$ Doped $TiO_2$ &Visible Light

pH is an important parameter for reactions taking place on the surface of a particulate, as is the case of $TiO_2$ photocatalysis.

### 4.3.1 Effect of pH for undoped $TiO_2$ and under visible light irradiation

The effect of solution pH was studied in the range of 2 to 10 for the optimized catalyst amounts (*i.e.*, 1 $gl^{-1}$) and visible light times (up to 180 min) for the azo dyes under study. Figure 4.15 shows the variation on the efficiency photocatalytic degradation of RB 5 at different pH values.

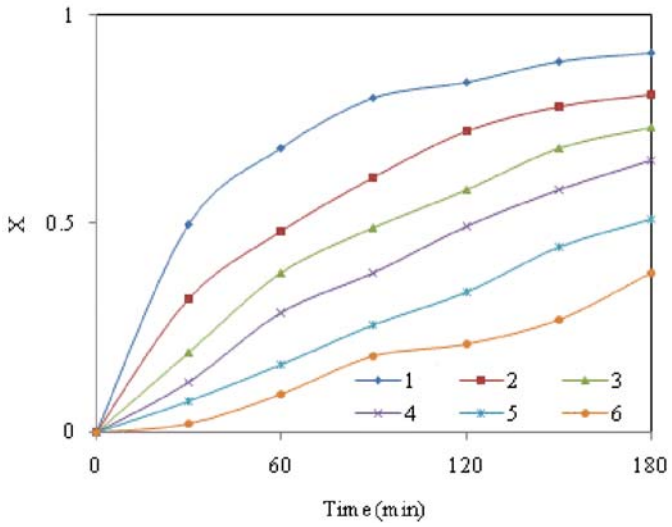


**Figure 4.15:** Effect of pH on photodegradation efficiency of RB 5 under visible light at the irradiation time of 3 h. Co = 100 ppm, $TiO_2$= 1 $gl^{-1}$ (1) pH = 2, (2) pH = 4, (3) pH = 6, (4) pH = 7, (5) pH = 8, (6) pH = 10

Photodegradation was higher in acidic media pH 2, 4 and 6 with degradation rates of 91, 81 and 73%, respectively. Up to a pH value of 8, the dye degradation decreased to 51%. Above pH 7, the degradation continued to decrease to about 38% at pH 10.

### 4.3.2 Effect of pH for 2 % Fe doped $TiO_2$ and under visible light irradiation

The effect of solution pH was studied in the range of 2 to 10 for the optimized catalyst (2 % Fe doped $TiO_2$) amounts (*i.e.*, 1 $gl^{-1}$) and visible light times (up to 180 min) for the azo dyes under study. Figure 4.16 shows the variation on the efficiency of photocatalytic degradation of RB 5 at different pH values. Photodegradation was higher in acidic media pH 2, 4 and 6 with degradation rates of 99, 98 and 95%, respectively. Up to a pH value of 8, the dye degradation decreased to 72%. Above pH 7, the degradation continued to decrease to about 51% at pH 10.

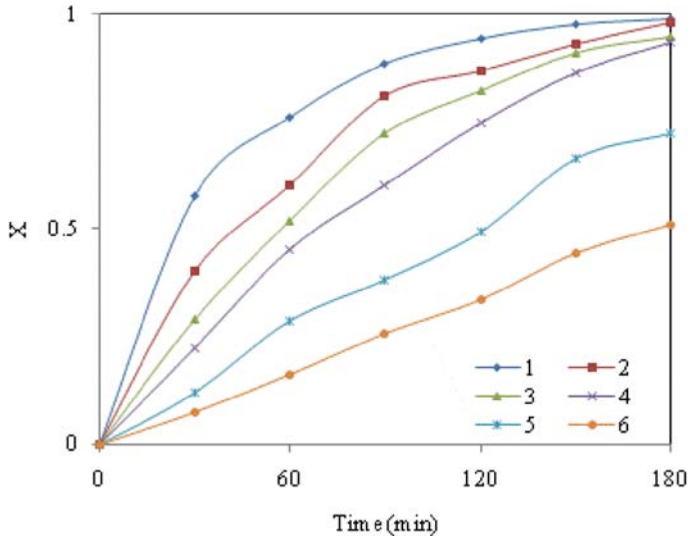


**Figure 4.16:** Effect of pH on photodegradation efficiency of RB 5 under visible light at the irradiation time of 3 h. Co = 100 ppm, 2 % Fe doped $TiO_2$= 1 $gl^{-1}$ (1) pH = 2, (2) pH = 4, (3) pH = 6, (4) pH = 7, (5) pH = 8, (6) pH = 10

### 4.3.3 Effect of pH for 4 % Fe doped $TiO_2$ and under visible light irradiation

The effect of solution pH was studied in the range of 2 to 10 for the optimized catalyst (4 % Fe doped $TiO_2$) amounts (*i.e.*, 1 $gl^{-1}$) and visible light times (up to 180 min) for the azo dyes under study. Figure 4.17 shows the variation on the efficiency of photocatalytic degradation of RB 5 at different pH values. Photodegradation was higher in acidic media pH 2, 4 and 6 with degradation rates of 99.9, 99 and 96%, respectively. Up to a pH value of 8, the dye degradation decreased to 79%. Above pH 7, the degradation continued to decrease to about 54% at pH 10.

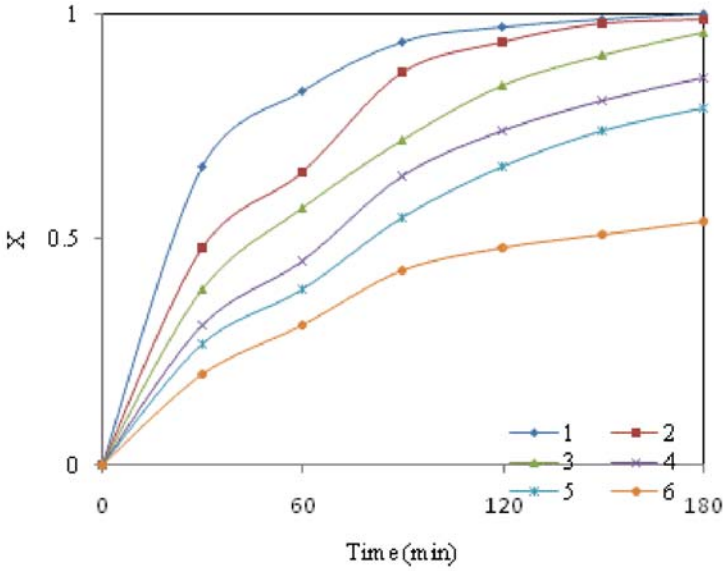


**Figure 4.17:** Effect of pH on photodegradation efficiency of RB 5 under visible light at the irradiation time of 3 h. Co = 100 ppm, 4 % Fe doped $TiO_2$= 1 $gl^{-1}$ (1) pH = 2, (2) pH = 4, (3) pH = 6, (4) pH = 7, (5) pH = 8, (6) pH = 10.

### 4.3.4 Effect of pH for 6 % Fe doped $TiO_2$ and under visible light irradiation

The effect of solution pH was studied in the range of 2 to 10 for the optimized catalyst (6 % Fe doped $TiO_2$) amounts (*i.e.*, 1 $gl^{-1}$) and visible light times (up to 180 min) for the azo dyes under study.

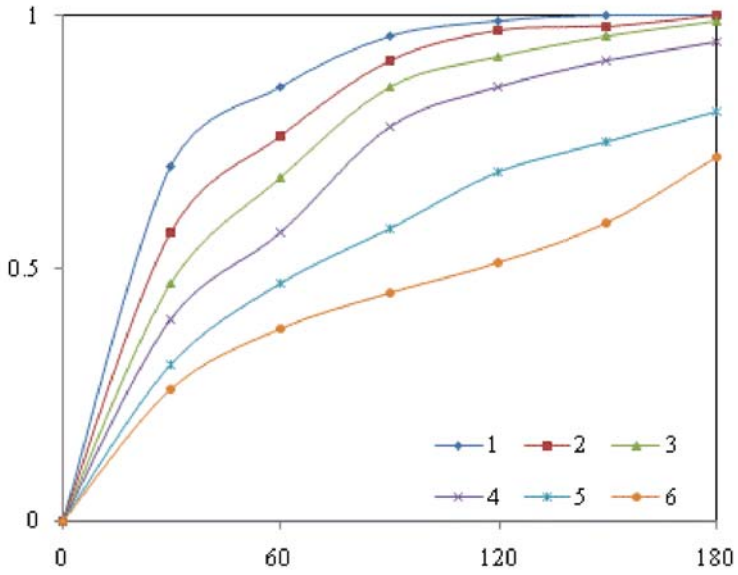


**Figure 4.18:** Effect of pH on photodegradation efficiency of RB 5 under visible light at the irradiation time of 3 h. Co = 100 ppm, 6 % Fe doped $TiO_2$= 1 $gl^{-1}$ (1) pH = 2, (2) pH = 4, (3) pH = 6, (4) pH = 7, (5) pH = 8, (6) pH = 10.

Figure 4.18 shows the variation on the efficiency photocatalytic degradation of RB 5 at different pH values. Photodegradation was higher in acidic media pH 2, 4 and 6 with degradation rates of 99.9, 99.9 and 99%, respectively. Up to a pH value of 8, the dye degradation decreased to 81%. Above pH 7, the degradation continued to decrease to about 72% at pH 10.

# Chapter-5

# CONCLUSIONS

From the present study the following conclusions have been made:

**Photodegration of dye under UV light and undoped $TiO_2$**

1. The optimum parameters were found to be $TiO_2$ dose = 1 $gl^{-1}$, initial dye concentration = 100 ppm and pH = 6, which showed 95 % dye degradation.
2. At optimum conditions, first order kinetic fitted the data, and the reaction rate constant was found to be 0.0127 $min^{-1}$.
3. The dye degradation in first, second, third, fourth, fifth and sixth reuse cycle were found to be 95, 87, 80, 75, 69 and 63 %, respectively.

**Doping of $Fe^{3+}$ ions over $TiO_2$ photocatalyst**

1. The XRD pattern of $Fe^{3+}$ ions over $TiO_2$ photocatalyst showed that the morphology of $TiO_2$ has not changed due to calcination at 500 $^{O}$C.
2. The width of peak at 25.4$^{O}$ did not change. It is showing that the particle size did not change during the modification of $TiO_2$ for different doping amount of $Fe^{3+}$ ions.
3. The SEM-EDS results showed that $Fe^{3+}$ ions was successively doped on the $TiO_2$ photocatalyst and $Fe^{3+}$ ions in Fe-$TiO_2$ were 1.86, 3.75 and 5.37 weight % $Fe^{3+}$ for 2, 4 and 6 weight % $Fe^{3+}$ ions dopant.

**Photodegradation of dye under visible light and $Fe^{3+}$ ions doped $TiO_2$**

1. The degradation was found to be 73 % for undoped $TiO_2$ for 100 ppm initial dye concentration, 1 $gl^{-1}$ $TiO_2$ photocatalyst dose and pH = 6.
2. The degradation was found to be 73, 95, 96 and 99 % for 2, 4 and 6 % $Fe^{3+}$ ions doped $TiO_2$, respectively, for 100 ppm initial dye concentration, 1 $gl^{-1}$ $TiO_2$ photocatalyst dose and pH = 6.

# REFERENCES


Adesina, A. A., Industrial exploitation of photocatalysis: progress, perspectives and prospects. Catalysis Surveys from Asia, 2004, 8 (4) 265 - 273.

Alaton, I. A. and Balcioglu, I. A., Photochemical and heterogeneous photocatalytic degradation of waste vinylsulphone dyes: a case study with hydrolysed Reactive Black 5, J. Photochem. Photobiol. A Chem., 2001, 141, 247-254.

Alekabi, H., and Serpone, N., Kinetic-studies in heterogeneous photocatalysis: 1: photocatalytic degradation of chlorinated phenols in aerated aqueous- solutions over $TiO_2$ supported on a glass matrix, J. Phys. Chem., 1988. 92 (20) 5726-5731.

Anpo, M. and Takeuchi, M., The design and development of highly reactive titanium oxide photocatalysts operating under visible light irradiation. J. Cat., 2003. 216, 505-516.

Anpo, M., Ichihashi, Y., Takeuchi, M. and Yamashita H., Design of unique titanium oxide photocatalysts by an advanced metal ion-implantation method and photocatalytic reactions under visible light irradiation, Res. Chem. Intermed., 1998. 24, 143-149.

Anpo, M., Shima, T., and Kubokawa, Y., ESR and photoluminescence evidence for the photocatalytic formation of hydroxyl radicals on small $TiO_2$ particles, Chemistry Letters, 1985, 1799-1802.

Asahi, R, Morikawa, T, Ohwaki, T, Aoki, K, Taga, Y., Visible-light photocatalysis in nitrogen-doped titanium dioxide, Science 2001, 293, 269-271.

Augugliaro, V., Palmisano, L., and Sclafani, A., Photocatalytic degradation of phenol in aqueous titanium dioxide dispersions, Toxicol. Environ. Chem., 1988, 16, 89-109.

Bahnemann, D., Bockelmann, D., and Goslish, R., Mechanistic studies of water detoxification in illuminated $TiO_2$ suspensions, Solar Energy Materials, 1991, 24, 564-583.

Bangun, J., and Adesina, A. A., The photodegradation kinetics of aqueous sodium oxalate solution using $TiO_2$ catalyst. Applied Catalysis A: General, 1998, 175, 221-235.

Bickley, R. I., and Stone, F. S., Photoadsorption and photocatalysis at rutile surfaces: I. Photoadsorption of oxygen. Journal of Catalysis, 1973. 31(3) 389-397.

Bizani E., Fytianos K., Poulios I. and Tsiridis V., Photocatalytic decolourization and degradation of dye solutions and wastewaters in the presence of titanium dioxide. J. Haz. Mat. 2006, 136 85-94.

Blake, D.M., Bibliography of work on the heterogeneous photocatalytic removal of hazardous compounds from water and air (National renewable energy laboratory), Golden, Colorado 2001.

Blake, D.M., ed. Bibliography of Work on Heterogeneous Photocatalytic Removal of Hazardous Compounds, US Department of Energy: Golden Colorado, 1995.

Blazkova, A., Csolleova, I., and Brezova, V., Effect of light sources on the phenol degradation using $Pt/TiO_2$ photocatalysis immobilized on glass fibres. J. Photochem. Photobio. A-Chem., 1998. 113(3) 251-256.

Braslavasky, S.E., and Houk, K.N., Glossary of terms used in photochemistry. Pure Appl. Chem., 1988. 60, 1055-1106.

Cao G., Li, Y., Zhangc, Q., Wanga, H., Synthesis and characterization of $La_2O_3/TiO_{2-x}F_x$ and the visible light photocatalytic oxidation of 4-chlorophenol, J. Haz. Matt., 2010, 178, 440–449.

Carneiro J O, Teixeira V, Portinha A, Dupak L, Magalhaes A, Coutinho P. Study of the deposition parameters and Fe-dopant effect in the photocatalytic activity of $TiO_2$ films prepared by dc reactive magnetron sputtering, Vacuum 2005, 78, 37-46.

Carraway, E. R., Hoffman, A. J., and Hoffman, M. R., Photocatalytic oxidation of organic acids on quantum-sized semiconductor colloids. Environ. Sci. Technol., 1994. 28, 786-793.

Carter S.R., Stefan M.I., Bolton J.R., Safarzadeh-Amiri A., $UV/H_2O_2$ treatment of methyl tertbutyl ether in contaminated waters, Environ. Sci. Technol, 2000, 34, 659-662.

Chen, L.C., and Chou, T.C., Kinetics of photodecolorization of methyl orange using titanium dioxide as catalyst. Ind. Eng. Chem. Res., 1993. 32, 1520-1527.

Choi, W., Termin, A., and Hoffmann, M. R., The role of metal ion dopants in quantum-sized tio2: correlation between photoreactivity and charge carrier recombination dynamics. J. Phys. Chem., 1994. 98, 13669-13679.

Colombo, J. D. P., and Bowman, R. M., Does interfacial charge transfer compete with charge carrier recombination? A femtosecond diffuses reflectance investigation of $TiO_2$ nanoparticles, J. Phys. Chem., 1996. 100, 18445-18449.

Colombo, J. D. P., and Bowman, R. M., Femtosecond diffuse reflectance spectroscopy of $TiO_2$ powders. J. Phys. Chem., 1995. 99, 11752-11756.

Colombo, P. D., Roussel, K. A., Saeh, J., Skinner, D. E., Cavaleri, J. J., and Bowman, R. M., Femtosecond study of the intensity dependence of electronhole dynamics in TiO2 nanoclusters. Chem. Phy. Lett., 1995, 232(3) 207-214.

Cong Y., Zhang J. L., Chen F. and Anpo M., Photocatalytic performance of a visible light TiO2 photocatalyst prepared by a surface chemical modification process, J. Phys. Chem. C, 2007, 111, 10618-10624.

Cunningham, J., Al-Shayyed, G., Sedlak, P., Caffrey, Aerobic and anaerobic $TiO_2$-photocatalysed purifications of waters containing organic pollutants, J. Cat. Today, 1999, 53, 145-152.

Daneshvar N., Salari D. and Khataee A. R., Photocatalytic degradation of azo dye acid red 14 in water: investigation of the effect of operational parameters, J. Photochem. Photobiol. A Chem. 2003, 157, 111-116.

D'Oliveira, J. C., Minero, C., Pelizzetti, E., and Pichat, P., Photodegradation of dichlorophenol and trichlorophenol in $TiO_2$ suspension - kinetic effects of the position of CI atom and identification of intermediates. J. Photochem. Photobiol. A: Chem., 1993. 72, 261-267.

Dostanic, J. M., Loncarevic, D. R., Bankovic, P.T., Cvetkovik, O.G., Jovanovic, D.M., Mijin, D.Z., Influence of process parameters on the photodegradation of synthesized azo pyridine dye in $TiO_2$ water suspension under simulated sunlight, J. Environ. Sci. Health Part A Toxic/Hazard. Subst Environ. Eng, 2011, 46, 70-79.

Dvoranova, D., Brezova, V., Mazur, M., and Malati, M.A., Investigations of metal-doped titanium dioxide photocatalysts.App. Cat. B: Envi., 2002, 37, 91 - 105.

Eckenfelder, W. W., Industrial water pollution control (3rd ed. McGrawHill), ISBN 0-07-116275-5, Boston, EUA 2000.

Engweiler, J., J. Harf, and Baiker, A., $WOx/TiO_2$ Catalysts prepared by grafting of tungsten alkoxides: morphological properties and catalytic behavior in the selective reduction of NO by $NH_3$. J. Cat., 1996, 159 (2) 259-269.

Fox M. A. and Dulay M., Heterogeneous Photocatalysis, Chem. Rev., 1993, 93, 341-357.

Fujishima M., Rao T. N., Tryk D. A., Titanium dioxide photocatalysis, J. Photochem. Photobio. C: Photochem. Rev., 2000, 1-21.

Fujishima, A. and K. Honda, Electrochemical photolysis of water at a semiconductor electrode. Nature, 1972, 238(5358) 37-38.

Fujishima, A., Hashimoto, K., and Watanabe, T., Photocatalysis: fundamentals and applications, 1999, Tokyo: BKC Inc.

Galindo P., Jacques A., and Kalt, Photodegradation of the aminoazobenzene acid orange 52 by three advanced oxidation processes: $UV/H_2O_2$, $UV/TiO_2$ and $VIS/TiO_2$: Comparative mechanistic and kinetic investigations, J. Photochem. Photobio. A: Chem., 2000, 130, 35-47.

Gerishcer, H., and Heller, A., The role of oxygen in photooxidation of organic moleculs on semiconductor particles. J. of Physi. Chem., 1991, 95-103.

Gombac V., Rogatis L. De, Gasparotto A., Vicario G., Montini T., Barreca D., Balducci G., Fornasiero P., Tondello E. and Graziani M., $TiO_2$ nanopowders doped with boron and nitrogen for photocatalytic applications, Chem. Phys., 2007, 339, 111-123.

Grzechulska J., and Morawski A.W., Photocatalytic decomposition of azo-dye acid black 1 in water over modified titanium dioxide, Appl. Catal. B, 2002, 36, 45-51.

Gu DE, Yang, BC.and Hu Y. D., V and N co-doped nanocrystal anatase $TiO_2$ photocatalysts with enhanced photocatalytic activity under visible light irradiation, Catal. Commun., 2008, 9 (6), 1472-1476.

Haber, J., Manual on catalyst characterization. Pure Appl. Chem, 1991, 63, 1227-1246.

Hansch, C., Leo, C., and Taft, R.W., A survey of Hammett substituent constants and resonance and field parameters. Chem. Rev., 1991. 19, 165-195.

Hao H. and Zhang J., The study of iron (III) and nitrogen co-doped mesoporous $TiO_2$ photocatalysts: synthesis, characterization and activity, Microporous Mesoporous Mater., 2009, 121(1-3), 52-57.

Herrmann, J.M., Heterogeneous photocatalysis: fundamentals and applications to the removal of various types of aqueous pollutants. Catalysis Today, 1999. 53, 115-129.

Hoffmann M.R., Martin S.T., Choi W., Bahnemann D.W., Environmental applications of semiconductor photocatalysis, Chem. Rev. 1995, 95, 69-96.

Hsiao, C.-Y., Lee C.-L., and Ollis D.F., Heterogeneous photocatalysis: degradation of dilute solutions of dichloromethane ($CH_2Cl_2$), chloroform ($CHCl_3$), and carbon tetrachloride ($CCl_4$) with illuminated $TiO_2$ photocatalyst. J.Cat., 1983, 82(2) 418-423.

Huang D. G., Liao S. J., Zhou W. B., Quan S. Q., Liu L., He Z. J. and Wan J. B. Synthesis of samarium- and nitrogen-co-doped $TiO_2$ by modified hydrothermal method and its photocatalytic performance for the degradation of 4-chlorophenol . J. Phys. Chem. Solids, 2009, 70, 853.

Huang D., Liao S., Liu J., Dang Z. and Petrik L. Preparation of visible-light responsive N–F-codoped $TiO_2$ photocatalyst by a sol–gel-solvo-thermal method .J. Photochem. Photobiol., A, 2006, 184, 282.

Hufschmidt, D., Liu, L., Selzer, V. and Bahnemann, D., Photocatalytic water treatment: fundamental knowledge required for its practical application. Wat. Sci. Tech., 2004. 49(4) 135-140.

Huo Y., Jin, J. Zhu and Li H, Highly active $TiO_{2-x-y}n_xF_y$ visible photocatalyst prepared under supercritical conditions in $NH_4F$/EtOH fluid. Appl. Catal., B, 2009, 89, 543-550.

Ihara, T., Miyoshi, M., Iriyama, Y., Matsumoto, O., and Sugihara, S., Visible-lightactive titanium oxide photocatalys realized by an oxygen-deficient structure and by nitrogen doping, App. Cat. B: Env., 2003. 42, 403-409.

Ishibashi K., Fujishima A., Watanabe T., Hashimoto K., Quantum yields of active oxidative species formed on $TiO_2$ photocatalyst. J. Photochem. Photobiol. A: Chemistry, 2000. 134, 139- 142.

Iwasaki, M., Hara, M., Kawada, H., Tada, H., and Ito, S., Cobalt ion-doped $TiO_2$ photocatalyst response to visible light.J. Coll. Int. Sci., 2000. 224, 202 - 204.

Joshi, J. B., Shah, Y. T., and Parulekar, S. J. Engineering aspects of the treatment of aqueous waste streams, Ind. Chem. Eng. 1985, 37, 3-9.

Justicia, I., Ordejon, P., Canto, G., Mozos, J. L., Fraxedas, J., Battiston, G.A., Gerbasi, R., and Figueras, A., Designed self-doped titanium oxide thin films for efficient visible-light photocatalysis, Adv. Mater., 2002. 14 (19) 1399 - 1402.

Korosi L, and Dekany I, Preparation and investigation of structural and photocatalytic properties of phosphate modified titanium dioxide, Colloids Surf A 2006, 280, 146-154.

Lee M. S., Hong S. S., and Mohseni M. Synthesis of photocatalytic nanosized $TiO_2$-Ag particles with sol-gel method using reduction agent, J Mol. Cat. A., 2005, 242, 135-140.

Legrini, O., Oliveros, E., and Braun, A. M., Photochemical porcesses for water treatment, Chem. Rev., 1993, 93 (2) 671-698.

Lettmann C, Hildebrand K, Kisch H, Macyk W, and Maier W. Visible light photodegradation of 4-chlorophenol with a coke-containing titanium dioxide photocatalyst. Appl. Cat. B 2001, 32, 215-227.

Li D., Hishita S., Kolodiazhnyi T. and H. Haneda, Origin of visible-light-driven photocatalysis: A comparative study on N/F-doped and N–F-codoped $TiO_2$ powders by means of experimental characterizations and theoretical calculations. J. Solid State Chem., 2005, 178, 3293.

Li, J, J. Xu, W. Dai, H. Li and K. Fan. One-pot synthesis of twist-like helix tungsten–nitrogen-codoped titania photocatalysts with highly improved visible light activity in the abatement of phenol, Appl. Catal., B, 2008, 82, 233-243.

Li, X. Z., and Li, F. B., Study of $Au/Au_3$ + $TiO_2$ photocatalysts towards visible photooxidation for water and wastewater treatment. Env. Sci. Tech. 2001, 35, 2381-2387.

Li, X. Z., Li, F. B., The enhancement of photodegradation efficiency using Pt-$TiO_2$ catalyst. Chemosphere, 2002, 48, 1103-1111.

Linsebigler, A. L., Lu, G, Yates Jr., J. T., Photocatalysis on TiO2 surfaces: principles, mechanisms and selected rules, Chem. Rev., 1995, 95, 735-768.

Litter, M. I., Heterogeneous photocatalysis - transition metal ions in photocatalytic systems, App. Cat. B-Env., 1999. 23(2-3) 89-114.

Livraghi S., Elghniji K., Czoska A. M., Paganini M. C., Giamello E. and Ksibi M. Nitrogen-doped and nitrogen–fluorine-codoped titanium dioxide, Nature and concentration of the photoactive species and their role in determining the

photocatalytic activity under visible light, J. Photochem, Photobiol., A, 2009, 205, 93-97.

Malato S., Blanco J., Maldonado M. I., Fernández-Ibáñez P., Campos A., and Malato, S., Optimising solar photocatalytic mineralization of pesticides by adding inorganic oxidizing species; application to the recycling of pesticide containers, App. Cat. B: Env., 2000. 28(3-4) 163-174.

Malato S., Blanco J., Ritchter C., Braun B., Maldonado M.I., Enhancement of the rate of solar photocatalytic mineralization of organic pollutants by inorganic oxidizing species. Appl. Catal. B, 1998, 17, 347-356.

Mao, Y., Schoneich, C., and Asmus, K. D., Identification of organic acids and other intermediates in oxidative degradation of chlorinated ethanes on titania surfaces en route to mineralization: a combined photocatalytic and radiation chemical study. J. Phys. Chem., 1991, 95(24) 10080-10089.

Matthews, R. W., and McEvoy, S. R., A comparison of 254 nm and 350 nm excitation of TiO2 in simple photocatalytic reactors, J. Photochem. Photobiol. A: Chem., 1992, 66, 355-366.

Metcalf and Eddy, Wastewater engineering – treatment and reuse (4rd ed. McGrawHill), ISBN 0-07-124140X, Boston, EUA 2003.

Mills A., and Hunte. S. L., An overview of semiconductor photocatalysis, J. Photochem. Photobio. A: Chem., 1997, 108, 1-35.

Mills, A., Davies, R. H., and Worsley, D., Water purification by semiconductor photocatalysis, Chem. Soc. Rev., 1993. 22, 417 - 425.

Moser, J., Gratzel, M., Photoelectrochemistry with colloidal semiconductors; laser studies of halide oxidation in colloidal dispersions of $TiO_2$ and - $Fe_2O_3$ Helv, Chim. Act A, 1982, 65, 1436-1444.

Muruganandham, M., Shobana, N. and Swaminathan, M., Optimization of solar photocatalytic degradation conditions of Reactive Yellow 14 azo dye in aqueous $TiO_2$, J. Mol. Cat. A: Chem., 2005, 246, 154-161.

Muruganandham M., Sobana N., Swaminathan M., Solar assisted photocatalytic and photochemical degradation of Reactive Black 5, J. Hazard. Mater., 2006, 137, 1371-1376.

Nagaveni K., Sivalingam G. and Heged M. S., Solar photocatalytic degradation of dyes: high activity of combustion synthesized nano $TiO_2$. Appl. Cat. B: Env., 2004, 48, 83-93.

Nguyen, T., and Ollis, D.F., Complete heterogeneously photocatalyzed transformation of 1,1- and 1,2-dibromoethane to carbon dioxide and hydrogen bromide. J. Phys. Chem., 1984. 88, 3386-3388.

Obata K., Irie H. and Hashimoto K., Enhanced photocatalytic activities of ta, n co-doped $tio_2$ thin films under visible light chem. Phys., 2007, 339, 124.

Okamoto, K., Yamamoto, Y., Tanaka, H., and ITAYA, A., Kinetics of heterogeneous photocatalytic decomposition of phenol over anatase TiO2 powder. Bull. Chem. Soc. Jpn., 1985. 58(7) 2023-2028.

Ollis, D. F., Pellizzetti, E., and Serpone, N., Destruction of water contaminants. Environ. Sci. Technol., 1991. 25, 1523-1528.

Pan C. C. and Wu J. C. S. Visible-light response Cr-doped $TiO_{2-x}N_x$ photocatalysts, Mater. Chem. Phys., 2006, 100 (1) 102-107.

Paola A. D, Garcia-Lopez E, Marci G, Martin C, Palmisano L, Rives V, Venezia A. M., Surface characterization of metal ions $TiO_2$ photocatalysts: structure-activity relationship, Appl. Cat. B: Env. 2004, 48, 223-233.

Pareek, V. K., and Adesina, A. A., Handbook of Photochemistry and Photobiology, American Scientific Publishers, H.S. Nalwa, Editor. 2003, Stevenson Ranch: CA, 345 - 412.

Parra S., Sarria V., Malato S., Péringer P., Pulgarin C., Photochemical versus coupled photochemical–biological flow system for the treatment of two biorecalcitrant herbicides: metobromuron and isoproturon, App. Cat. B: Env., 2000, 27(3) 153-168.

Pitchat, P. and M. A. Fox, Photocatalysis on Semiconductors, in Photoinduced Electron Transfer (Part D), M.A. Fox and M. Chanon, Editors. 1988, Elsevier: New York. 241-302.

Poznyak, S. K., Talapin, D., and Kulak, A., structural, optical, and photoelectrochemical properties of nanocrystalline $TiO_2$-$In_2O_3$ composite solids and films prepared by sol-gel method, J. Phys. Chem. B, 2001, 105, 4816-4823.

Pruden, A. L. and D. F. Ollis, Photoassisted heterogeneous catalysis: the degradation of trichloroethylene in water. Journal of Catalysis, 1983, 82(2) 404-417.

Raphael, M. W., and Malati, M. A., The photocatalysed reduction of aqueous sodium carbonate using platinized titania. Journal of Photochemistry and Photobiology A: Chemistry, 1989. 46(3) 367-377.

Rodríguez O., González F., Bosch P., Portilla M., Viveros T., Physical characterization of $TiO_2$ and $Al_2O_3$ prepared by precipitation and sol-gel methods. Catalysis Today, 1992. 14, 243-252.

Rodrriguez-Talavera, R., Vargas, S., Arroyo-Murillo, R., Montiel-Campos, R., and Haro-Toniatowski, E., Modification of the phase transition temperatures in titania doped with various cations. J. Mater. Res., 1997. 12, 439-443.

Saggioro E. M., Oliveira A. S., Pavesi T., Maia C. G., Ferreira L. F. V. and Moreira J. C., Use of titanium dioxide photocatalysis on the remediation of model textile wastewaters containing azo dyes, Molecules, 2011, 16, 10370-10386.

Sakata, Y., Yamamoto, T., Okazaki, T., Imamura, H., and Tsuchiya, S., Generation of visible light response on the photocatalyst of a copper ion containing $TiO_2$. Chem. Lett., 1998. 12, 1253-1254.

Sauer T., Neto, G. C., José, H. J. and Moreira R. F. P. M., Kinetics of photocatalytic degradation of reactive dyes in a $TiO_2$ slurry reactor. Journal of Photochemistry and Photobiology A: Chemistry. 2002, 149, 147-154.

Schiavello, M., Basic Concepts in Photocatalysis, in Photocatalysis and environment: trends and applications, M. Schiavello, Editor. 1988, Kluwer Academic Publishers: Dordrecht, The Netherlands.

Serpone, N., Maruthamuthu, P., Pichat, P., Pelizzetti, E., and Hidaka, H., Exploiting the interparticle electron transfer process in the photocatalysed oxidation of phenol, 2-chlorophenol and pentachlorophenol: chemical evidence for electron and hole transfer between coupled semiconductors, Journal of Photochemistry and Photobiology A: Chemistry, 1995. 85(3) 247-255.

Shen X. Z., Liu Z. C., Xie S. M. and Guo J., Degradation of nitrobenzene using titania photocatalyst co-doped with nitrogen and cerium under visible light illumination, J. Hazard. Mater, 2009, 162 (2-3) 1193-1198.

Shen Y, T. Xiong, T. Li and K. Yang., Tungsten and nitrogen co-doped $TiO_2$ nano-powders with strong visible light response, Appl. Catal., B, 2008, 83, 177.

Tahiri, H., Ichou, Y. A., and Herrmann, J. M., Photocatalytic degradation of chlorobenzoic isomers in aqueous suspensions of neat and modified titania, Journal of Photochemistry and Photobiology A: Chemistry, 1998. 114 (3) 219-226.

Takeshita K, Yamakata A, Ishibashi T, Onishu H, Nishijima K, Ohno T. Transient IR absorption study of charge carriers photogenerated in sulfur-doped $TiO_2$, J Photochem. Photobiol., 2006, 177, 269-275.

Teichner, S. J., and Formenti, M., Photoelectrochemistry, Photocatalysis, and Photoreactors, M. Schiavello, Editor. 1985, D. Reidel Publishers: Dordrecht. p.457.

Toor A. P., Verma A., Jotshi C. K., Bajpai P. K. and Singh V., Photocatalytic degradation of Direct Yellow 12 dye using UV/$TiO_2$ in shallow pond slurry reactor, Dyes and Pigments, 2006, 68, 53-60.

Treschev S. Y., Chou P. W., Tseng T. H., Wang J. B., Perevedentseva E. V., Cheng C. L., Photoactivities of the visible light-activated mixedphase carbon-containing titanium dioxide: The effect of carbon incorporation. Appl. Cat. B 2008, 79, 8-16.

Trillas, M., Pujol, M., and Domenech, X., Phenol photodegradation over titanium dioxide, J. Chem. Technol. Biotechnol., 1992. 55, 85-90.

Turchi, C.S. and Ollis, D. F., Photocatalytic degradation of organic water contaminants: Mechanisms involving hydroxyl radical attack, J. of Cat., 1990. 122(1) 178-192.

Wang N., Li J., Zhu L., Dong Y. and Tang H., Highly photocatalytic activity of metallic hydroxide/ titanium dioxide nanoparticules prepared via a modified wet precipitation process, J. Photochem. Photobiol. A Chem, 2008, 198, 282-287.

Wang Q., Chen C., Ma W., Zhu H. and Zhao J., Pivotal role of fluorine in tuning band structure and visible-light photocatalytic activity of nitrogen-doped $TiO_2$, Chem.–Eur. J., 2009, 15(19), 4765-4769.

Wang, Y., Cheng, H., Zhang, L., Hao, Y., Ma, J., Xu, B., and Li, W., The preparation, characterization, photoelectrochemical and photocatalytic properties of lanthanide metal-ion-doped TiO2 nanoparticles, J.Mol. Cat. A: Chemi., 2000. 151, 205 - 216.

Wei H, Y. Wu, Lun N. and Zhao F., Preparation and photocatalysis of $TiO_2$ nanoparticles co-doped with nitrogen and lanthanum, J. Mater. Sci., 2004, 39(4), 1305.

Wei, T.Y., and Wan, C.C., Heterogeneous photocatalytic oxidation of phenol with titanium-dioxide powders, Ind. Eng. Chem. Res., 1991. 30(6) 1293- 1300.

Wilke, K., and Breuer, H. D., The influence of transition metal doping on the physical and photocatalytic properties of titania, J. Photochem. Photobio. A-Chem., 1999. 121(1) 49-53.

Wong, W.K., and Malati, M. A., Doped $TiO_2$ for solar-energy applications, Solar Energy, 1986. 36(2) 163-168.

Wu J. C-S, and Chen C. H., A visible-light response vanadium-doped titania nano-catalyst by sol-gel method, J. Photochem. Photobiol. A 2004, 163, 509-515.

Wu Z, Dong F, Zhao W, Guo S. Visible light induced electron transfer process over nitrogen doped $TiO_2$ nanocrystals prepared by oxidation of titanium nitride, J. Haz. Mat., 2008, 157 (1) 57-63.

Xie Y. and Zhao X., The effects of synthesis temperature on the structure and visible-light-induced catalytic activity of F–N-codoped and S–N-codoped titania, J. Mol. Catal. A: Chem., 2008, 285 (1-2), 142-149.

Xing M. Y., Zhang J. L. and Chen F., Photocatalytic performance of N-doped $TiO_2$ adsorbed with $Fe^{3+}$ Ions under visible light by a redox treatment, J. Phys. Chem. C, 2009, 113, 12848-12853.

Xu, A. W., Gao, Y., Liu, H. Q., The preparation, characterization, and their photocatalytic activities of rare-earth-doped TiO2 nanoparticles. J. Cat., 2002. 207(2) 151 - 157.

Xu, X. H., Wang, M., Hou, Y., Yao, W. F., Wang, D., and Wang, H., Preparation and characterization of Bi-doped $TiO_2$ photocatalyst, J. Mat. Sci. Let, 2002. 21, 1655 - 1656.

Yang, Y.; Li, X.-J.; Chen, J. T. and Wang, L.Y., Effect of doping mode on the photocatalytic activities of Mo/$TiO_2$. J. Photochem. Photobio. A: Chem.. 2004, 163, 517-522.

Yoneyama, H., Takao, Y., Tamura, H., Bard, A. J., Factors influencing product distribution in photocatalytic decomposition of aqueous acetic acid on platinized titania, J. Phys. Chem., 1983. 87, 1417-1422.

Zainal, Z., Hui, L. H., Hussein, M. Z. and Ramli, I., Removal of dyes using immobilized titanium dioxide illuminated by fluorescent lamps, J.Haz. Mat., 2005, 125, 113-120.

Zaleska A, Sobczak J. W., Grabowska E., Hupka J., Preparation and photocatalytic activity of boron-modified $TiO_2$ under UV and visible light, App. Cat. B 2007, 78, 92-100.

Zhang X. and Liu Q., Visible-light-induced degradation of formaldehyde over titania photocatalyst co-doped with nitrogen and nickel, Appl. Surf. Sci., 2008, 254, 4780-4785.

Zhou M, Yu J, Cheng B, Zhao X., Preparation, characterization and photocatalytic activity of in situ N, S-codoped $TiO_2$ powders, J Mol. Cat. A, 2006, 246, 176-184.

Zhou Y, Liu Q, Zhu Z, Zhang J., Preparation and properties of vanadium-doped $TiO_2$ photocatalysts, J. Phys. D: Appl. Phys., 2010, 43, 1-6.

Zielinska B., Grzechulska J., Grzmil B., Morawski A.W., Photocatalytic degradation of Reactive Black 5 A comparison between $TiO_2$-tytanpol A11 and $TiO_2$-degussa P25 photocatalysts, Appl. Catal. B, 2001, 35, L1-L7.